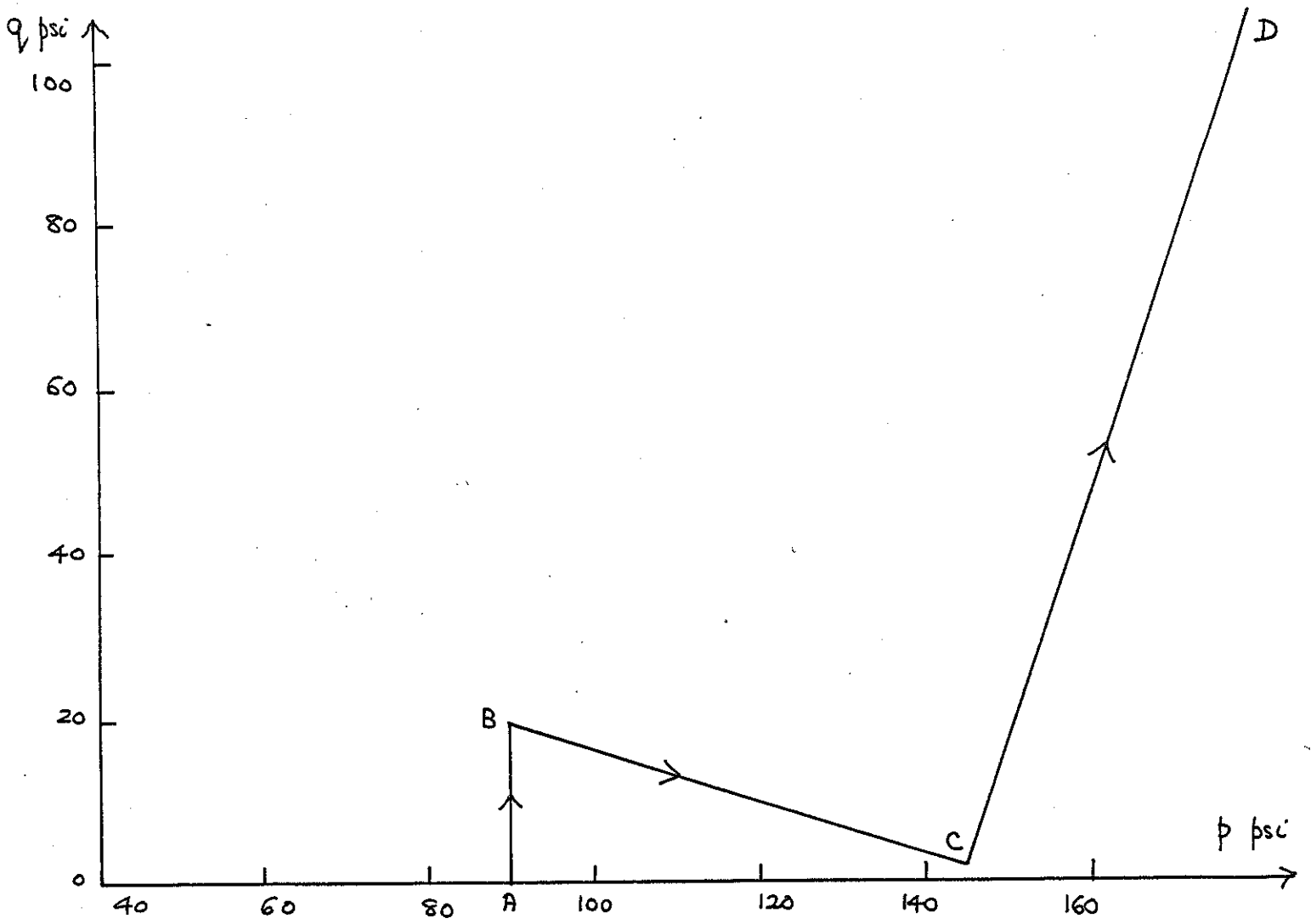

Fig. 6.67. The stress path followed by specimen CO.

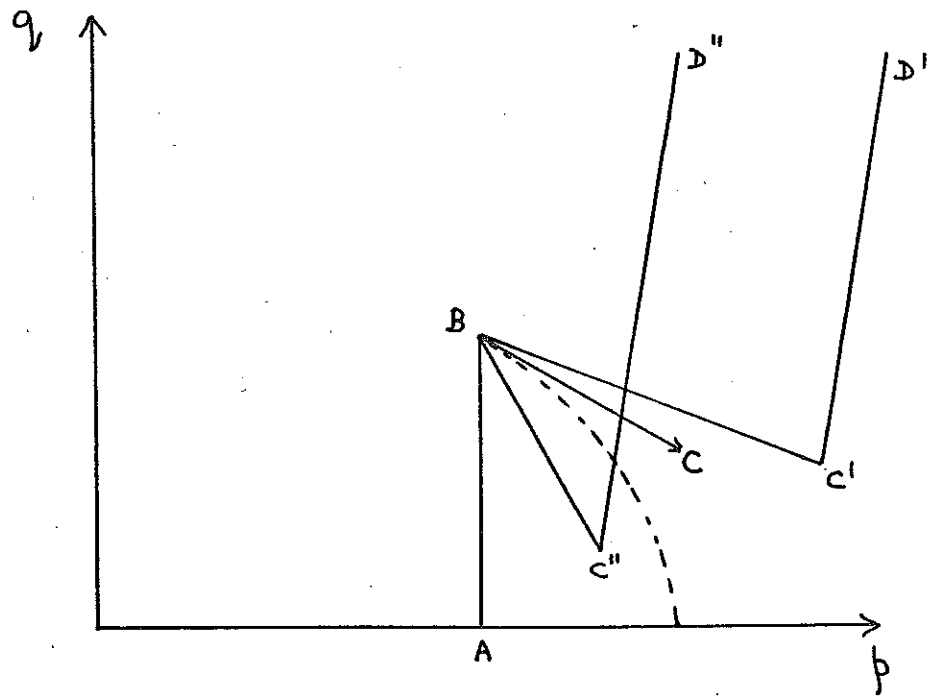

Fig. 6.67 (a). The reloading stress paths with states of specimen lying inside and on the state boundary surface.

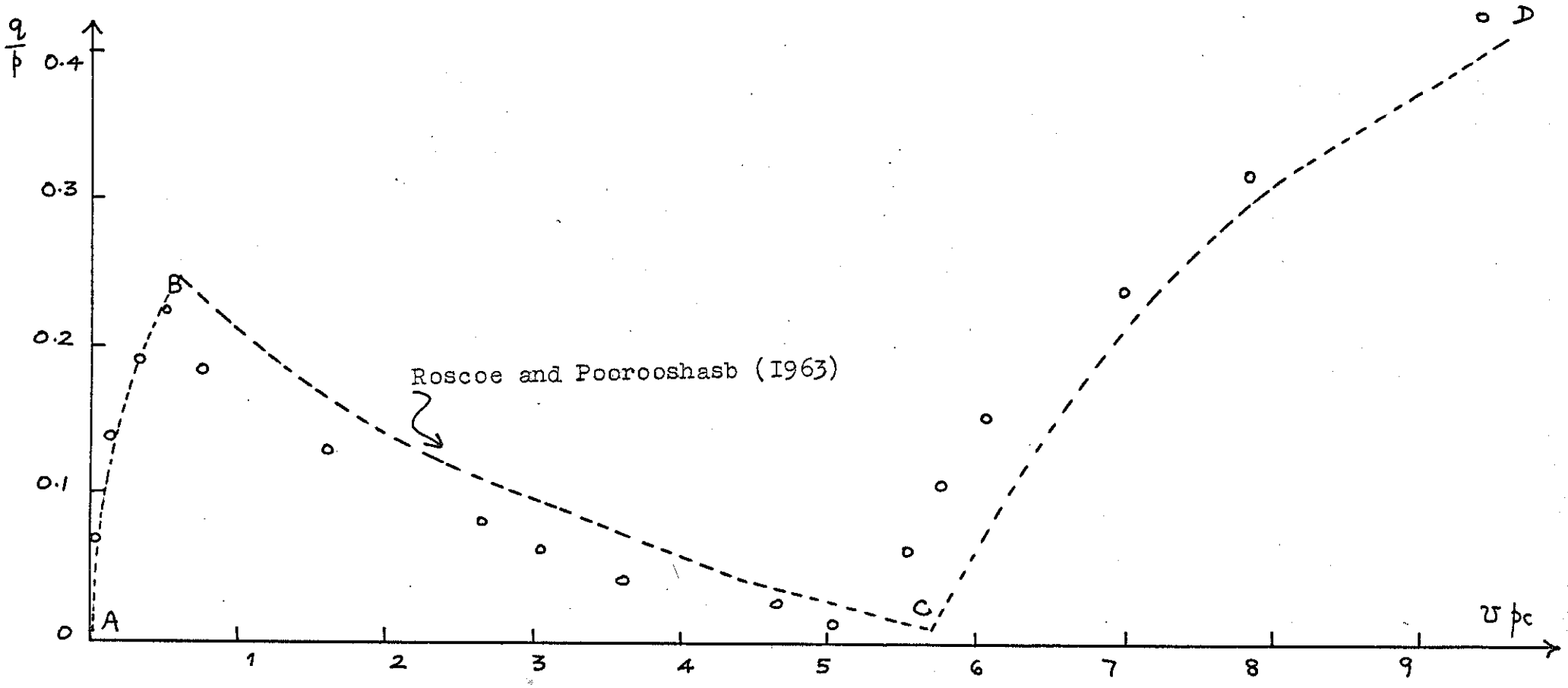

Fig.6.68. Observed and predicted strains on specimen CO

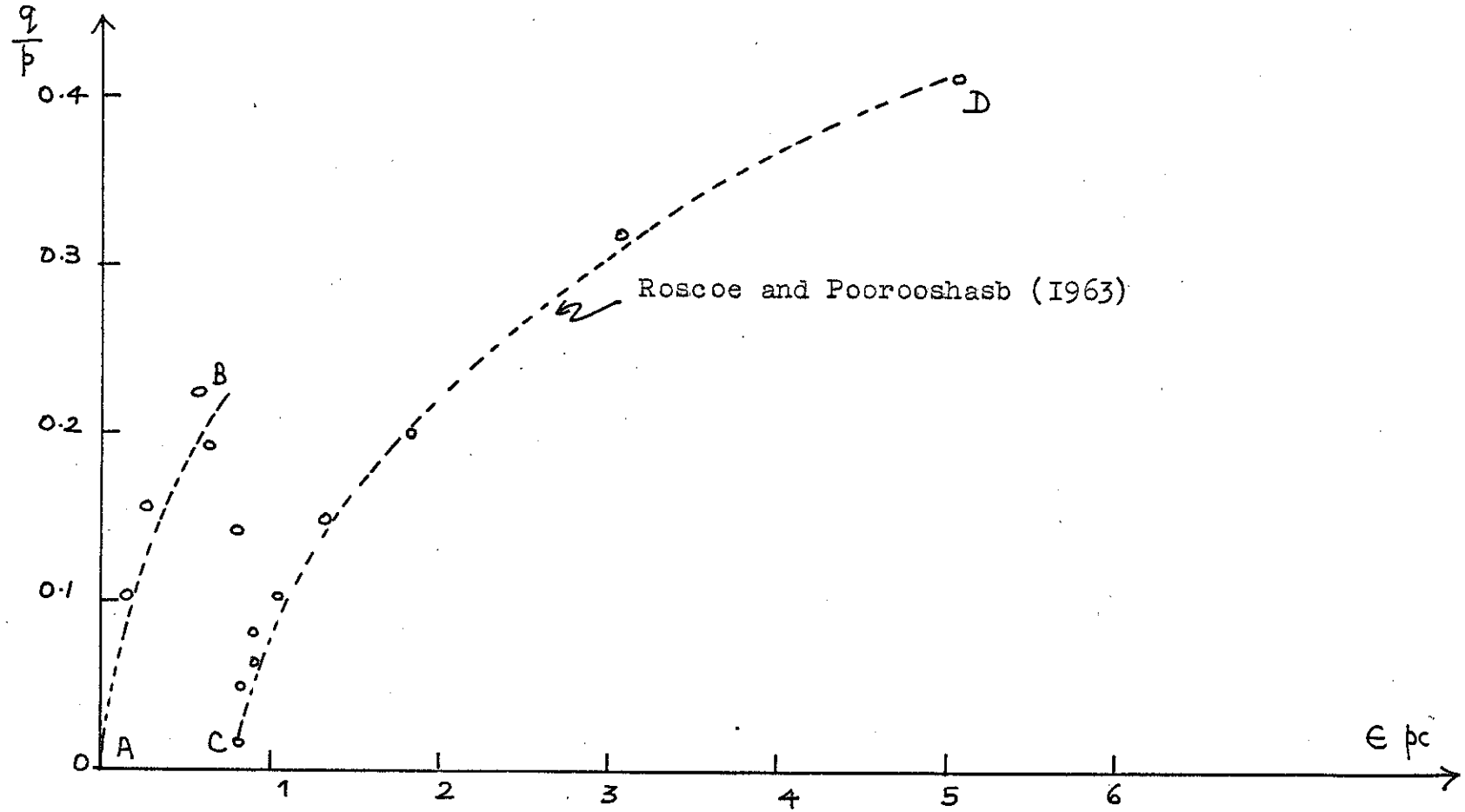

Fig.6.69. Observed strains and the predicted strains for the loading and reloading phase. Sample CO.

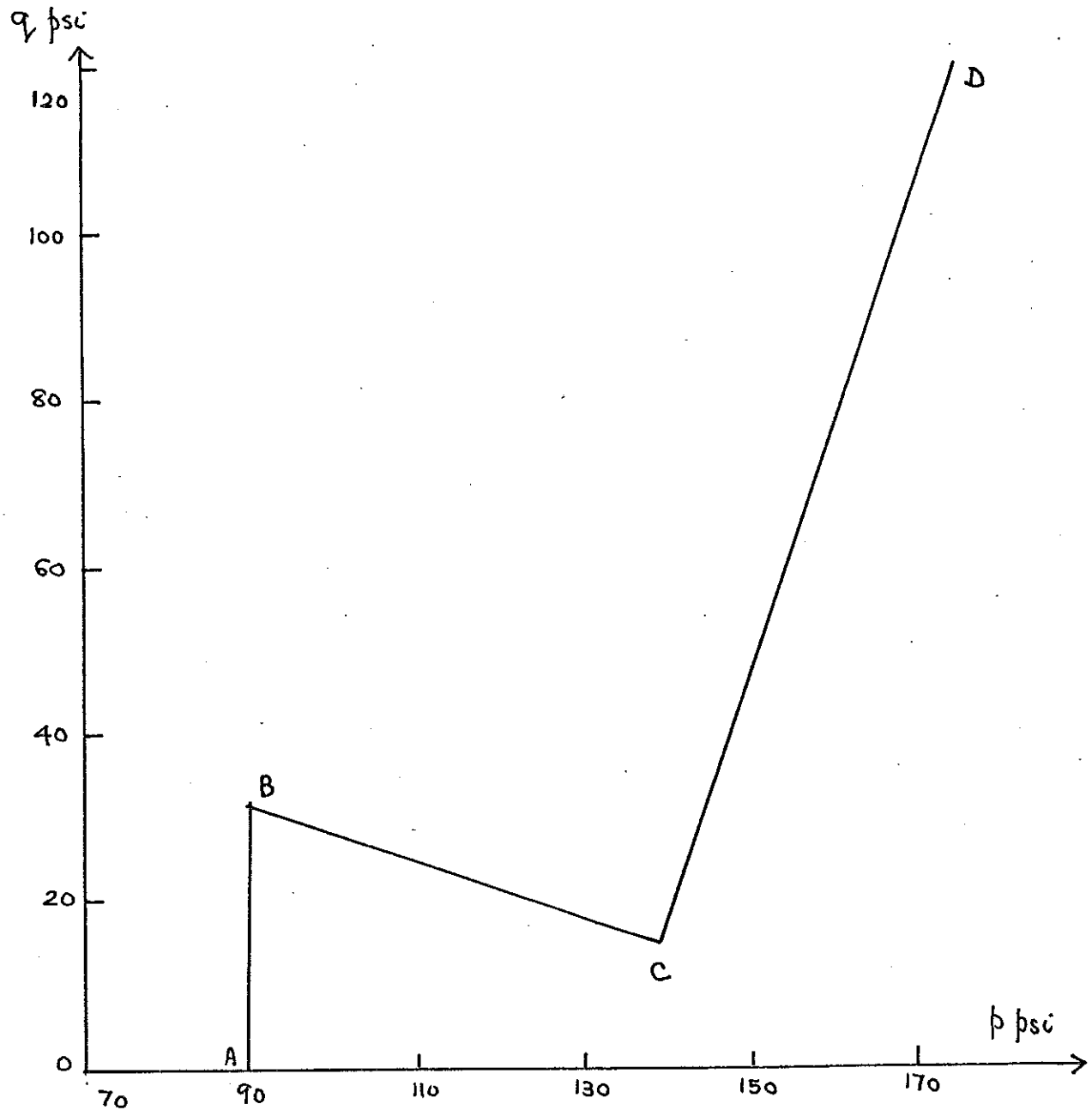

Fig. C.70. The stress path followed by specimen CL.

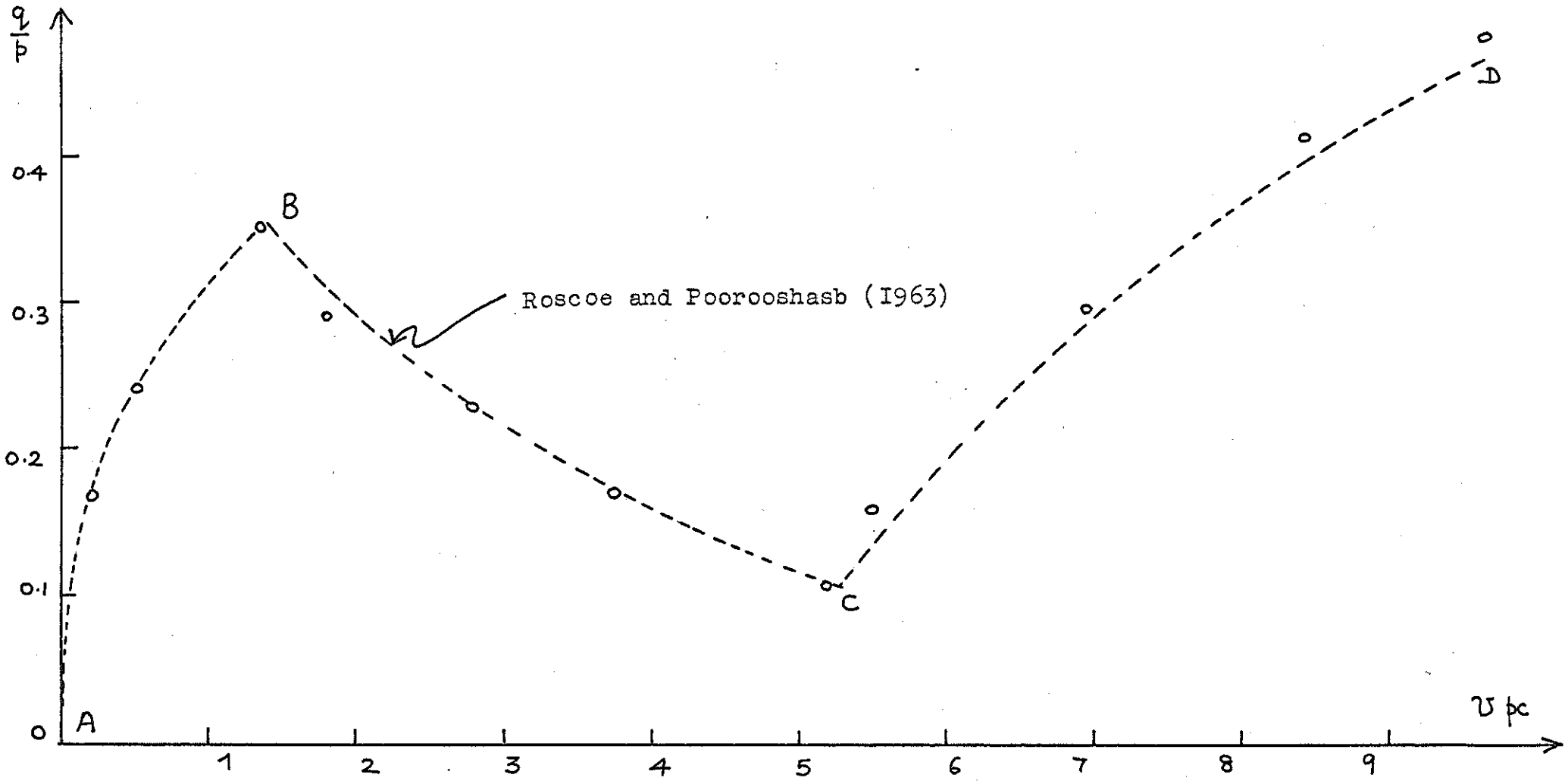

Fig. 6.71. Observed and predicted strains on sample CL.

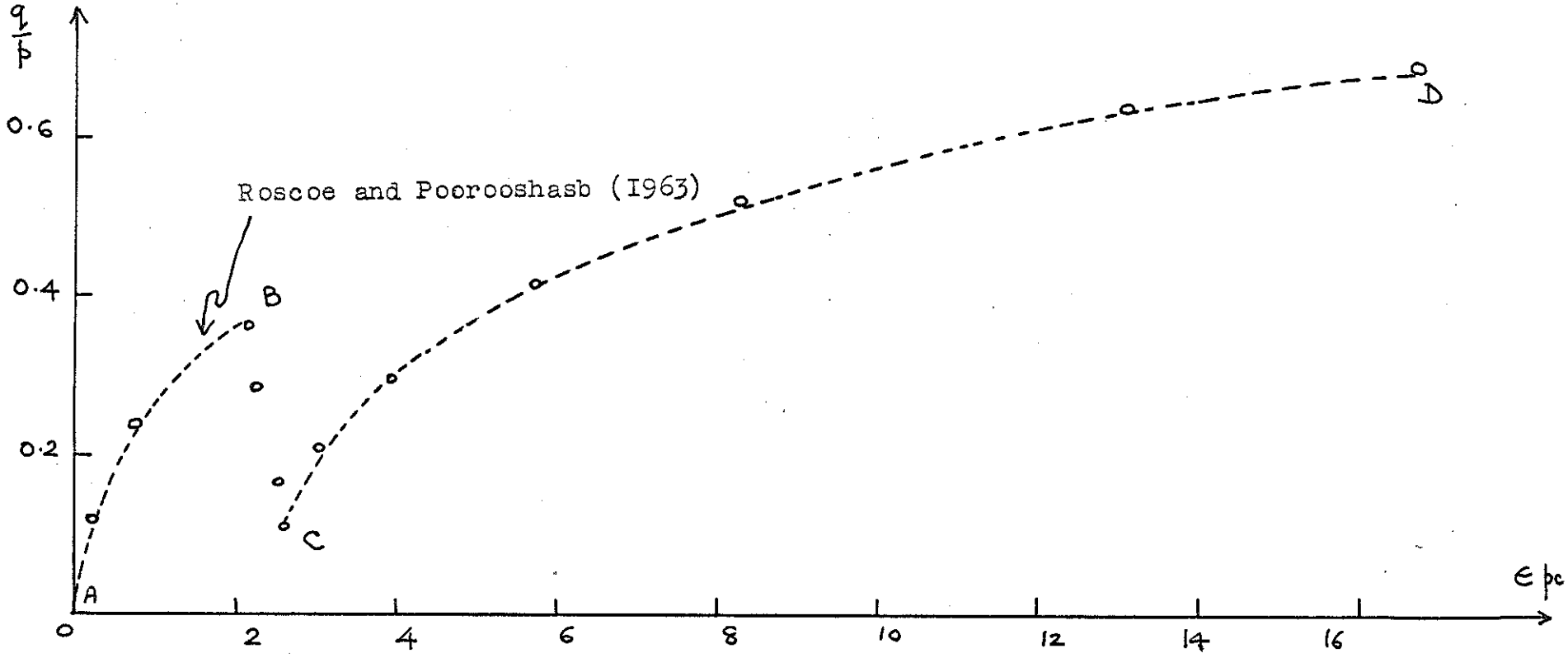

Fig.6.72. Observed shear strains and the predicted shear strains for the loading and reloading phase on sample CL.

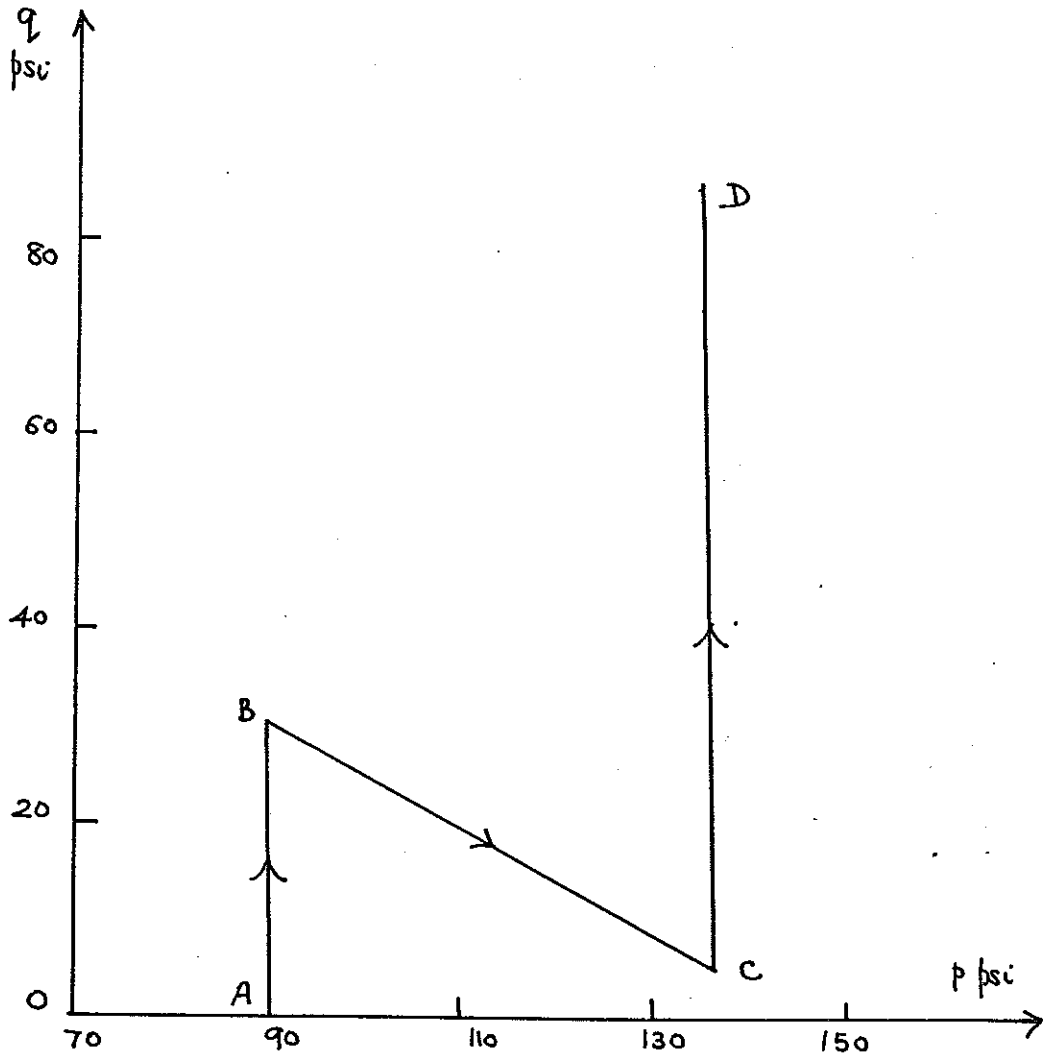

Fig. 6.73. The stress path followed by specimen BP.

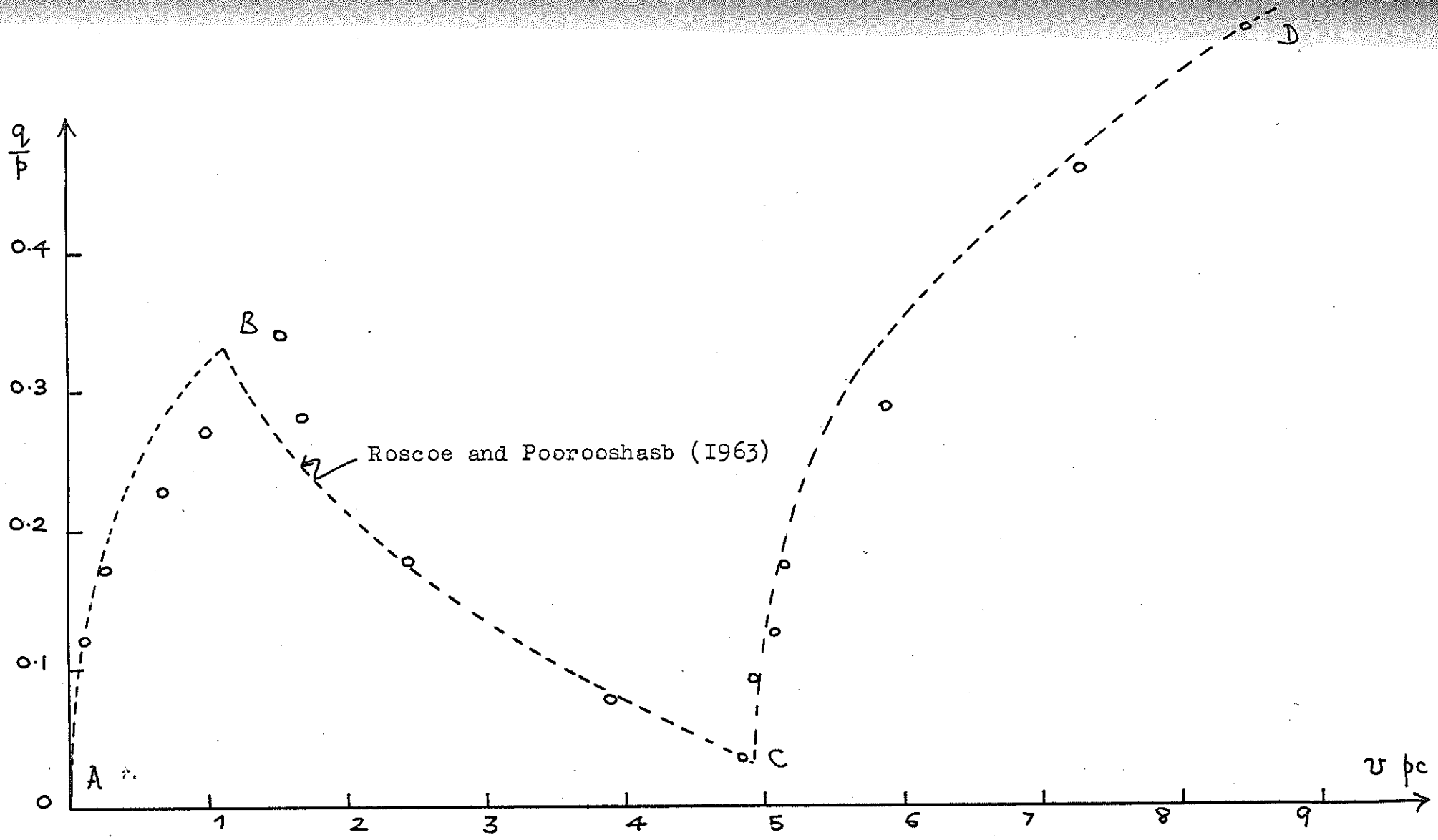

Fig. 6.74 Observed and predicted volumetric strains on sample BP.

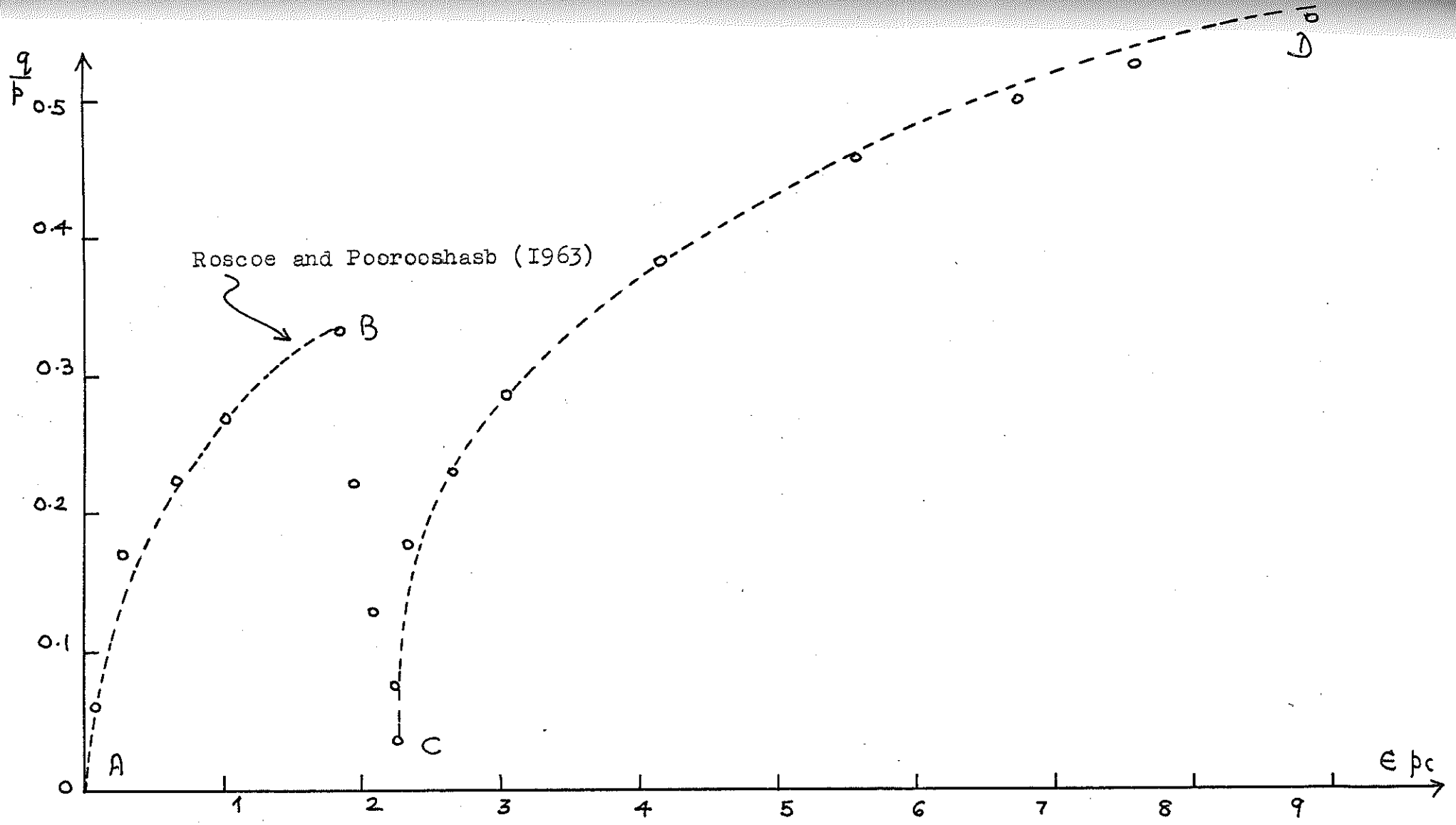

Fig. 6.75. Observed shear strains and the predicted shear strains for the loading and reloading phases on sample BP.

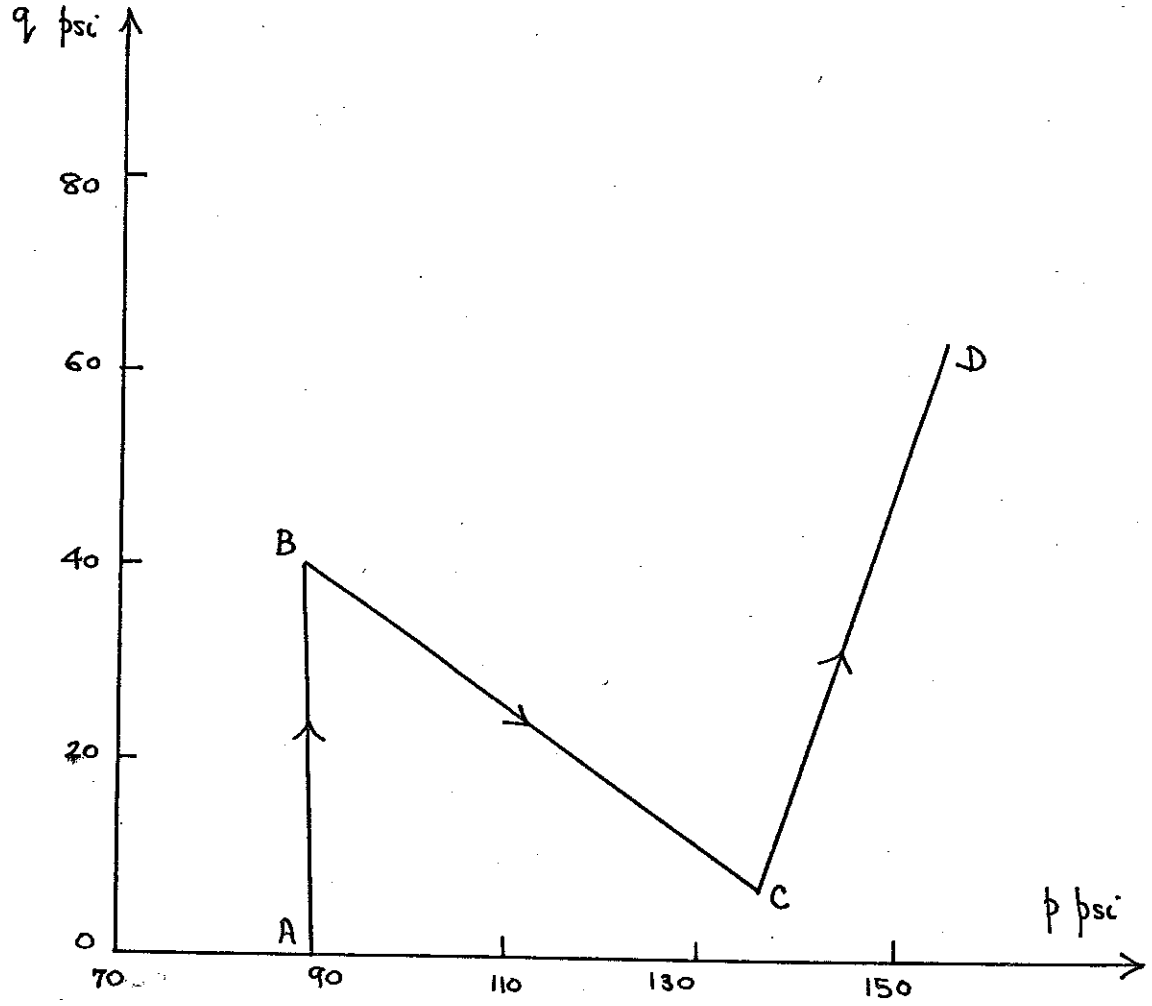

Fig. 6.76. The stress path followed by specimen CP.

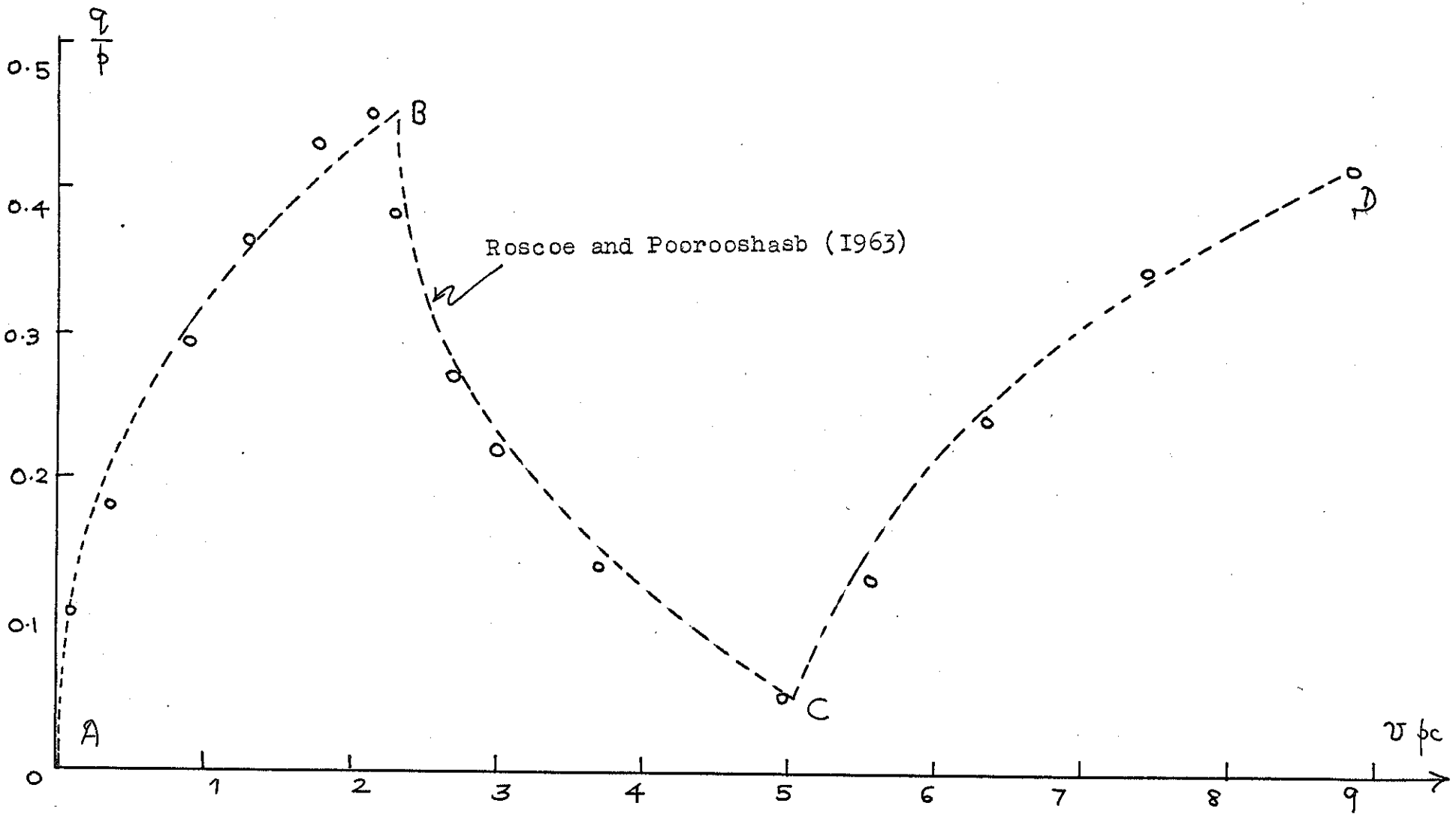

Fig. 6.77. Observed and predicted volumetric strains on sample CP.

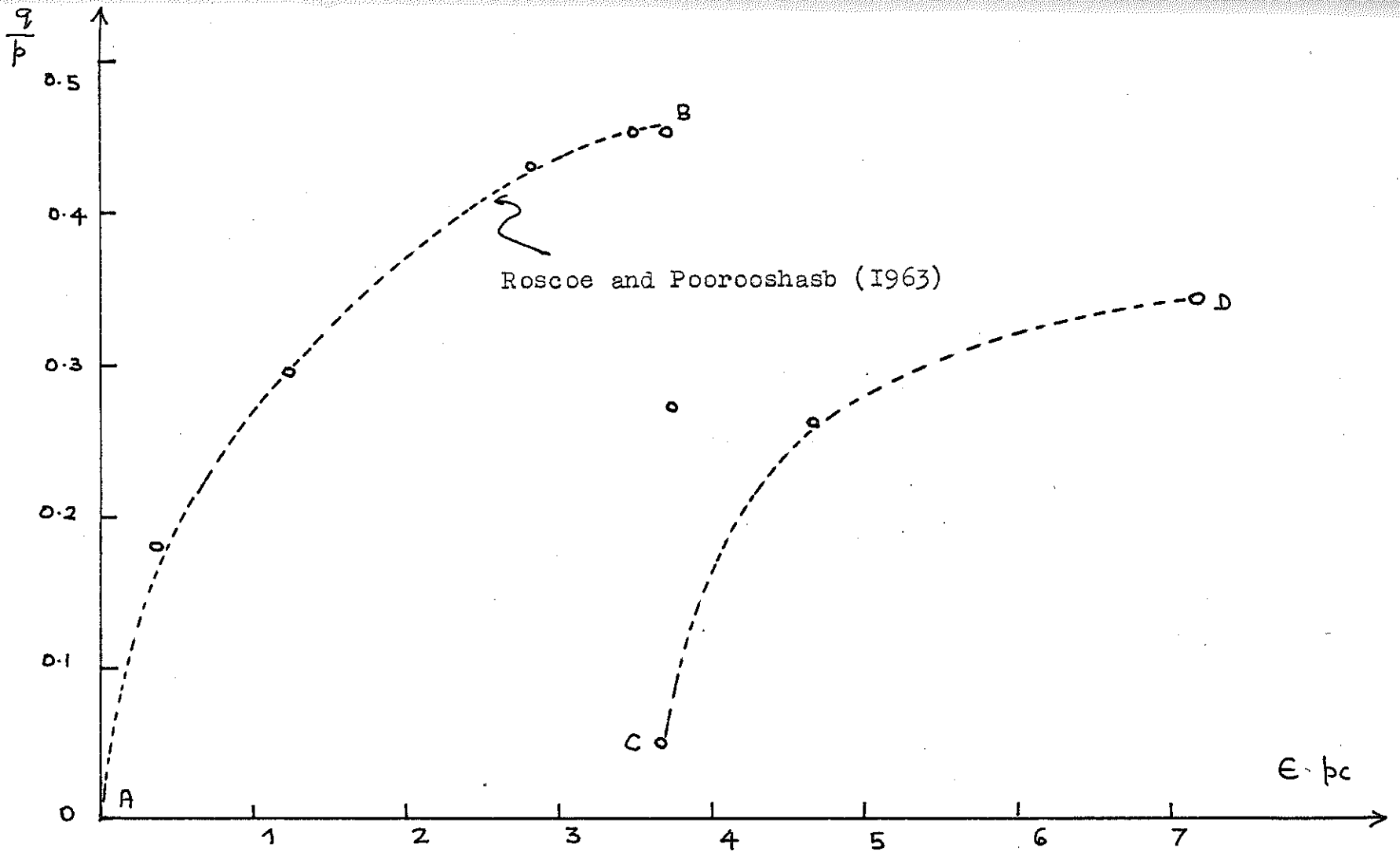

Fig. 6.78 Observed shear strains and the predicted shear strains for the loading and reloading phases on sample CP.

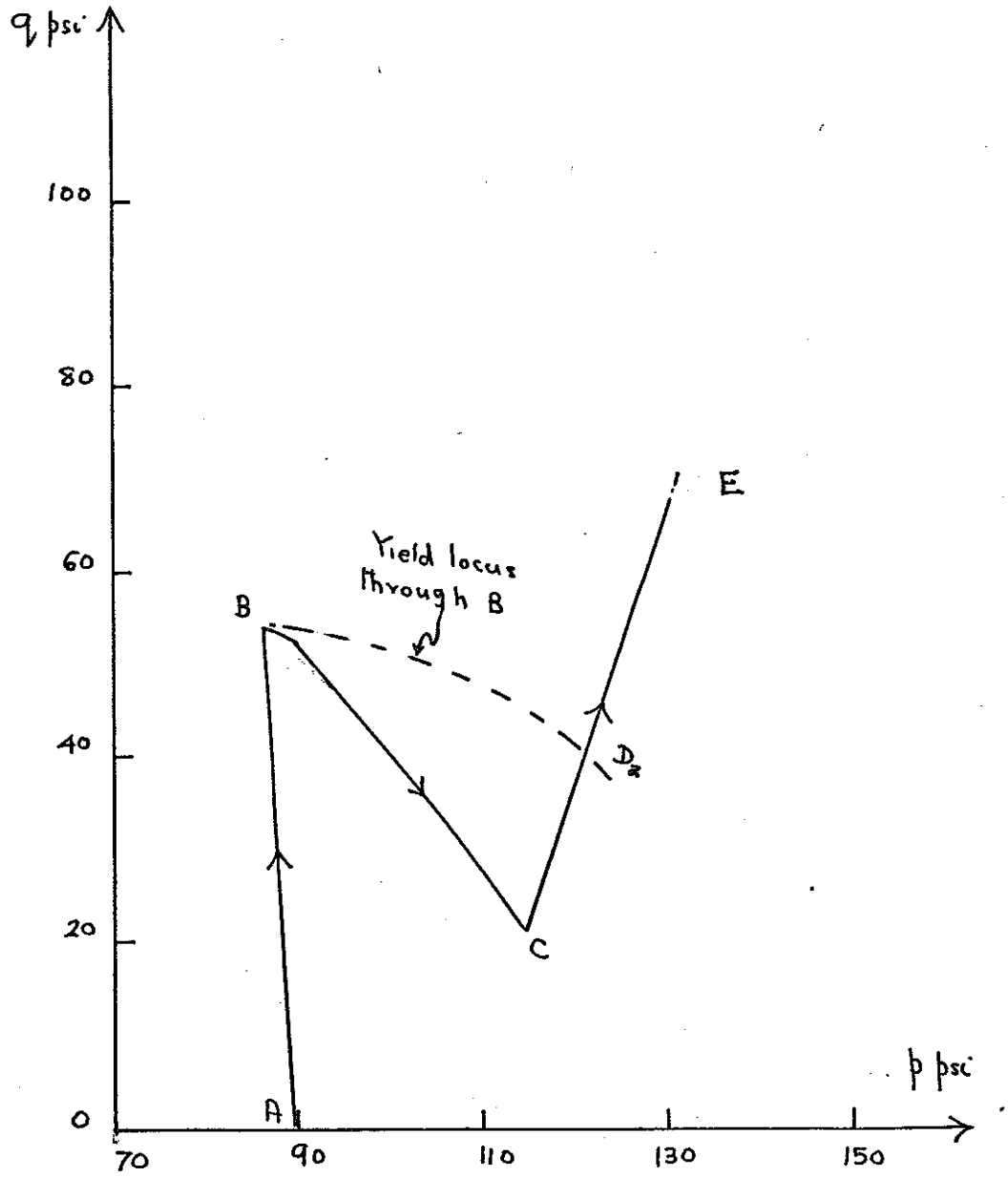

Fig. 6.79. Stress path followed by specimen CM

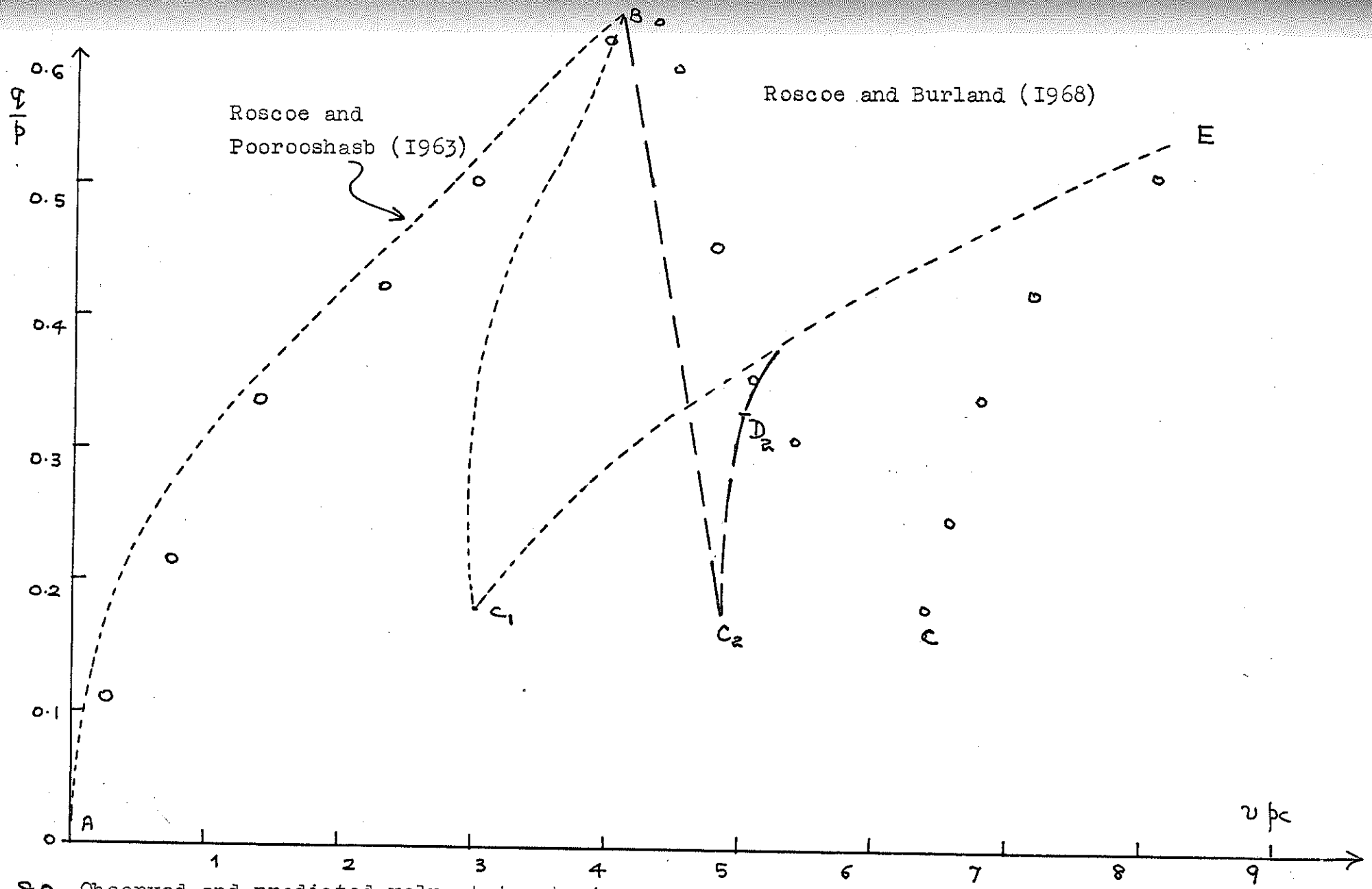

Fig. 6·80. Observed and predicted volumetric strains on sample CM.

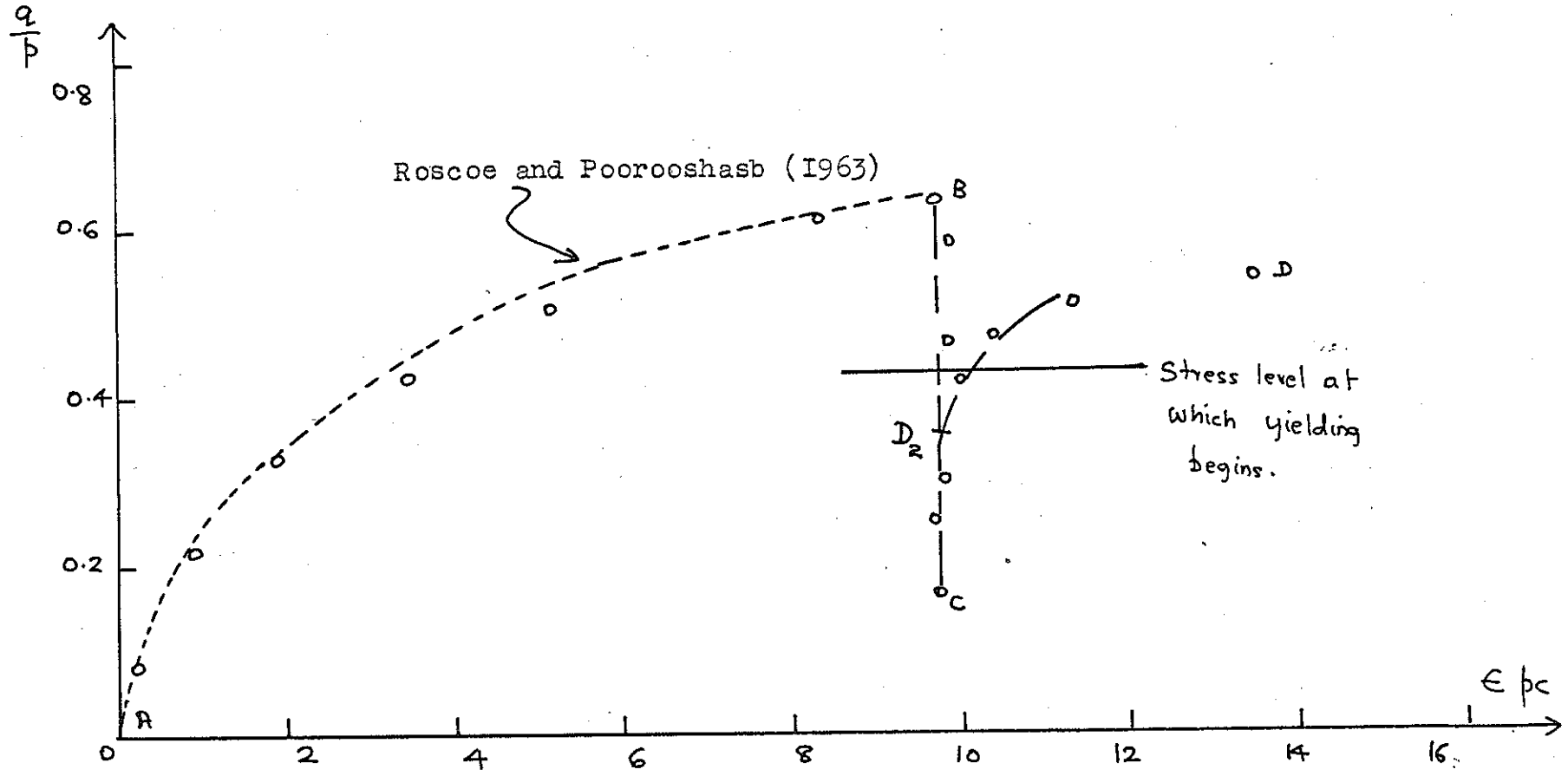

Fig. 6.81. Observed and predicted strains on sample CM.

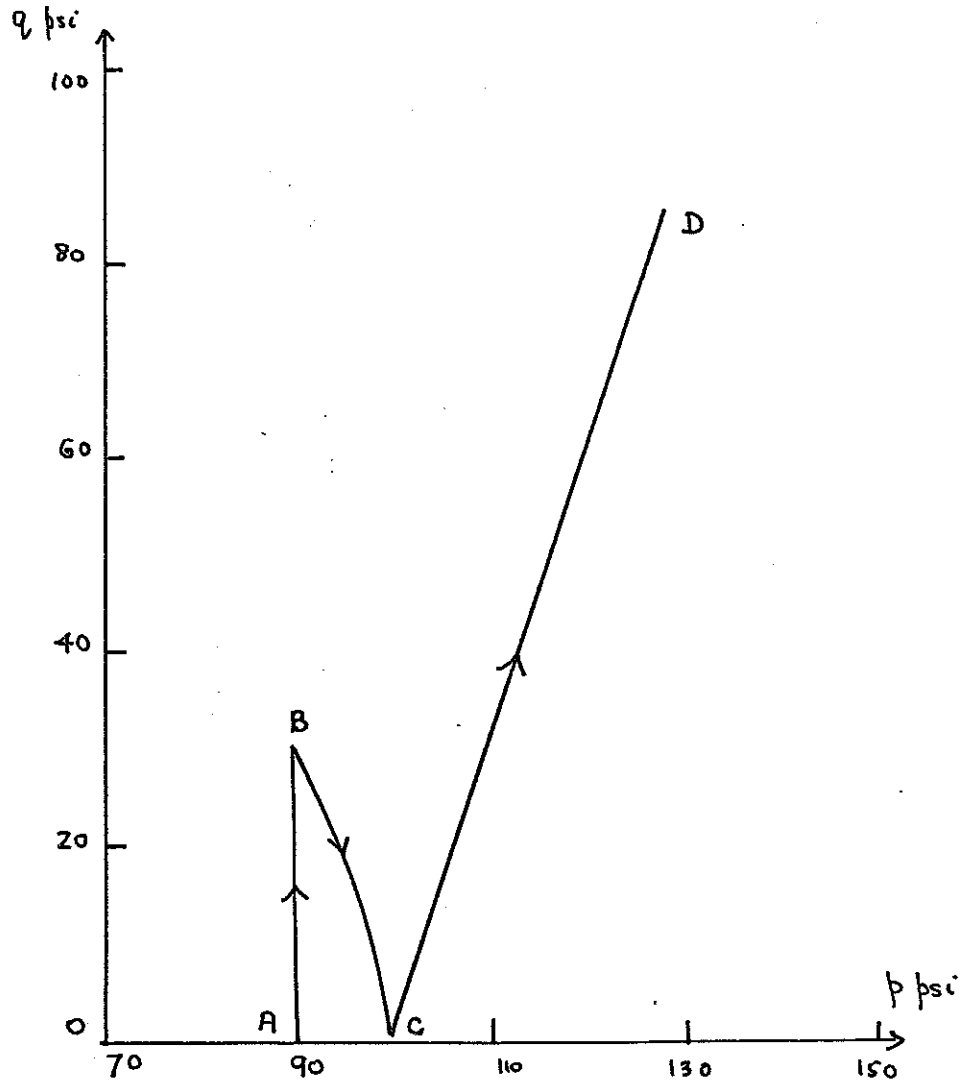

Fig. 6.82. The stress path followed by specimen BO.

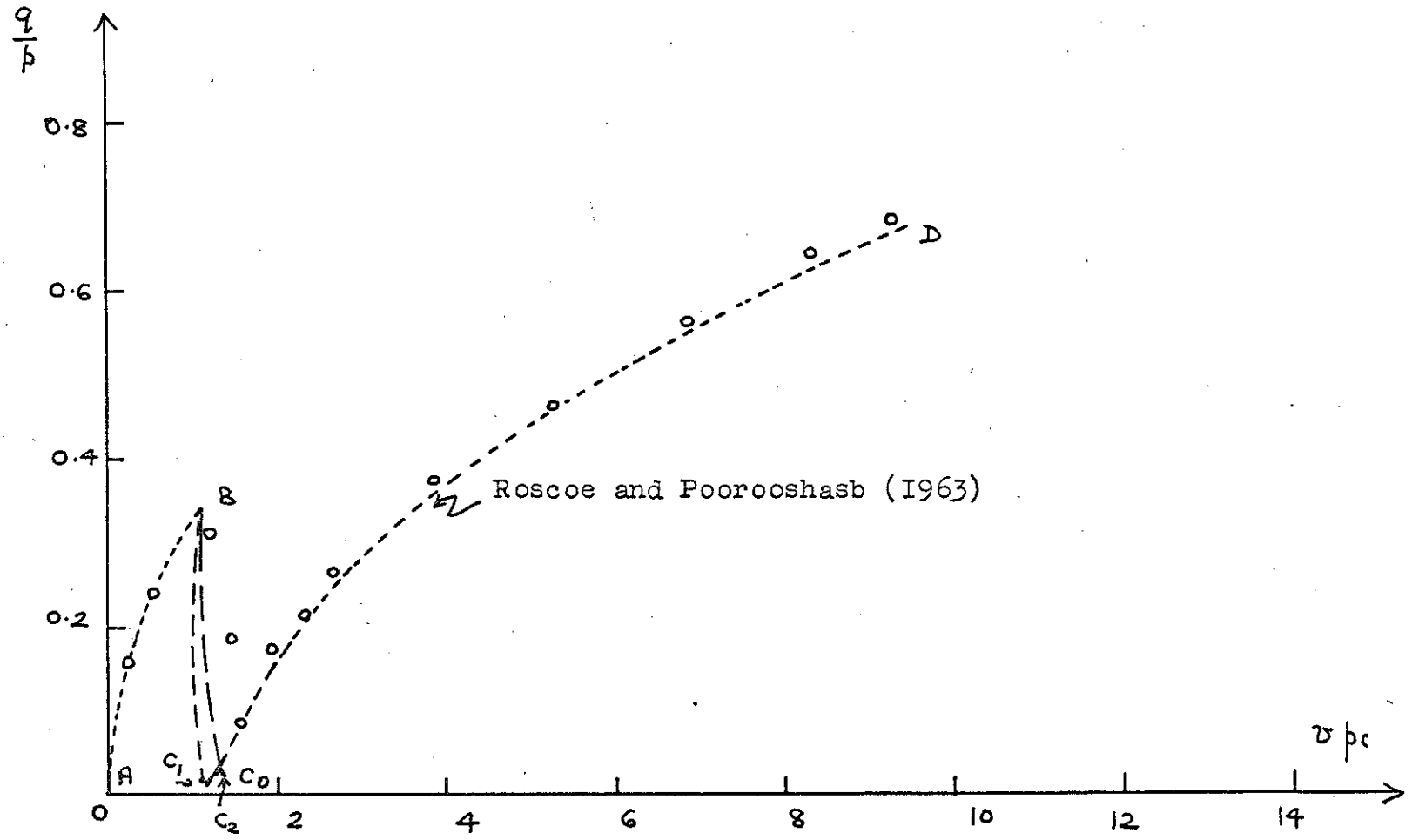

Fig. 6.83. Observed and predicted volumetric strains on sample BO.

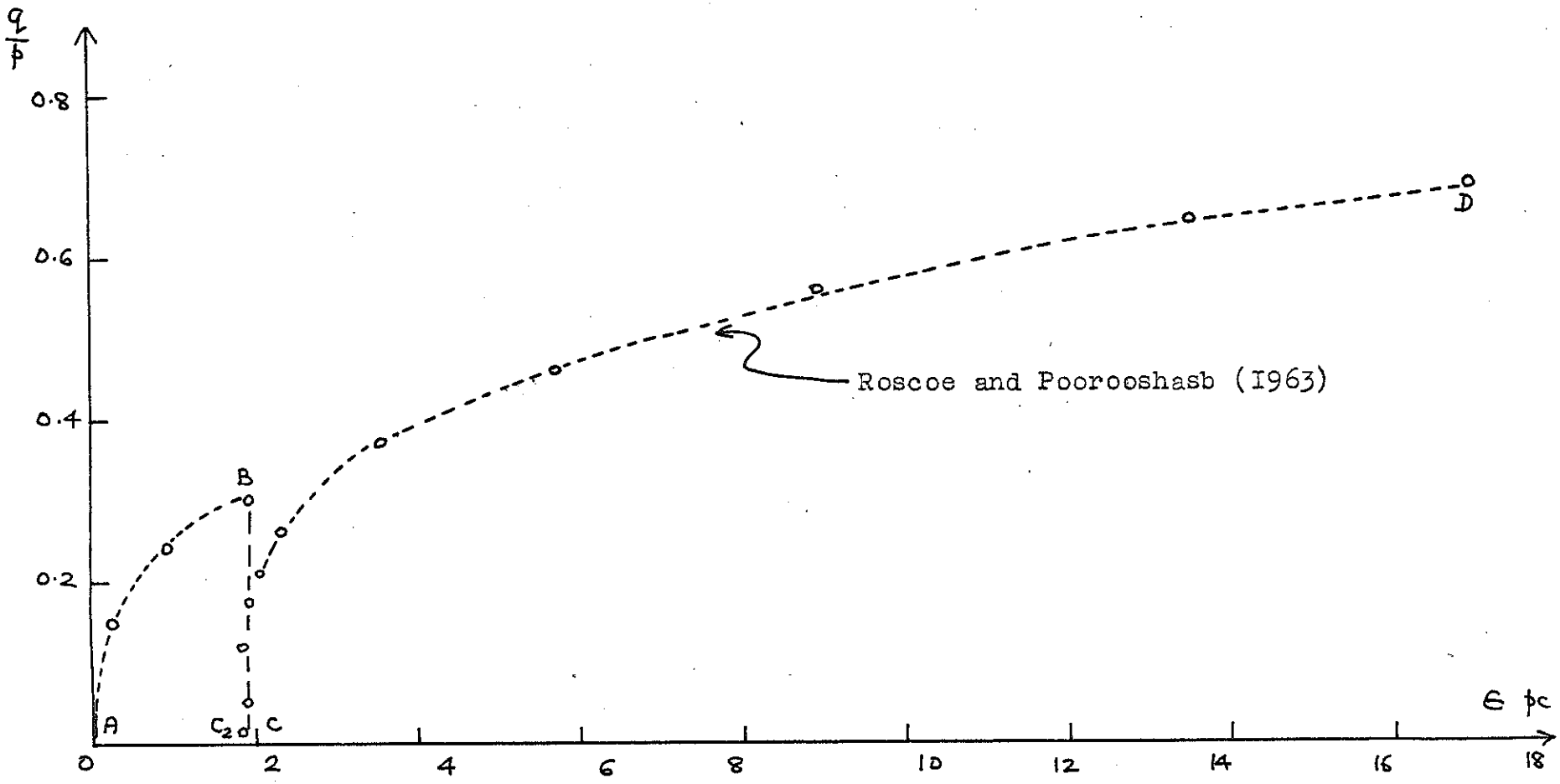

Fig. 6.84. Observed and predicted shear strains on sample BO.

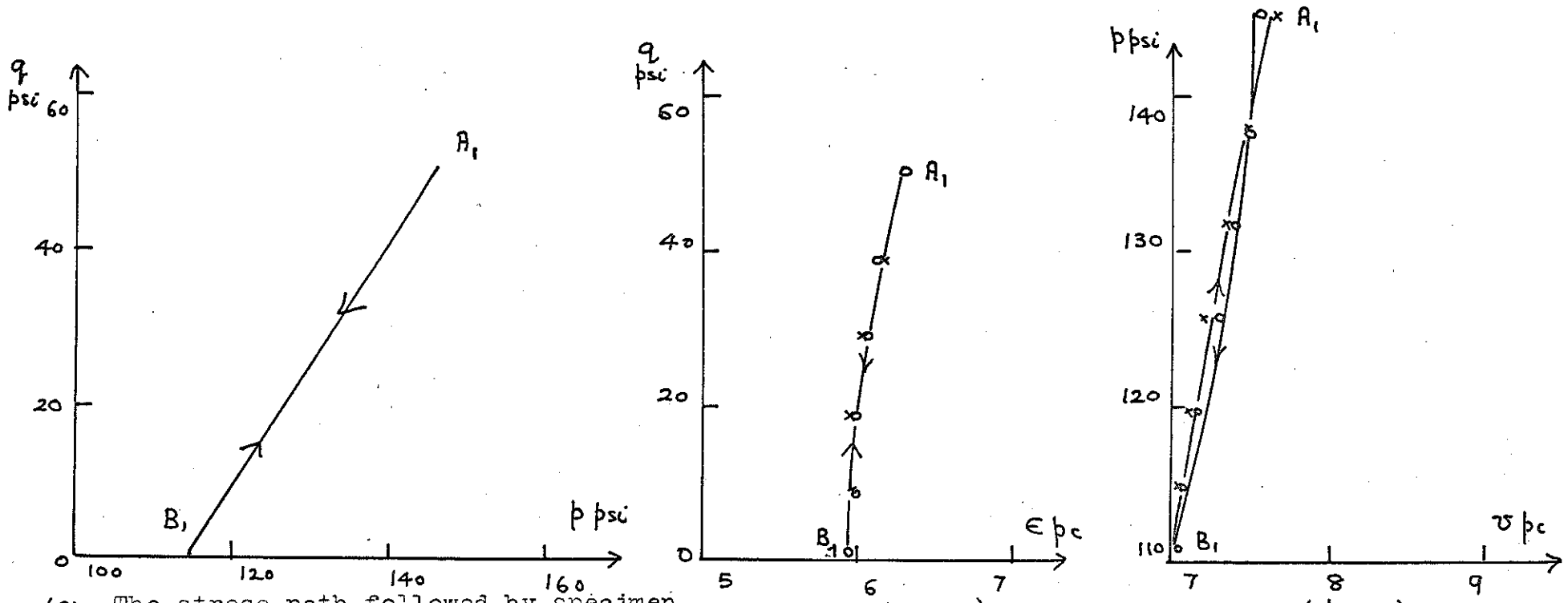

(a) The stress path followed by specimen CG during unloading.

(b) The (q , ϵ) relation

(c) The (p , v) relation.

Fig.6.85.The (q , ϵ) and (p , v) characteristics of specimen CG during unloading and reloading.

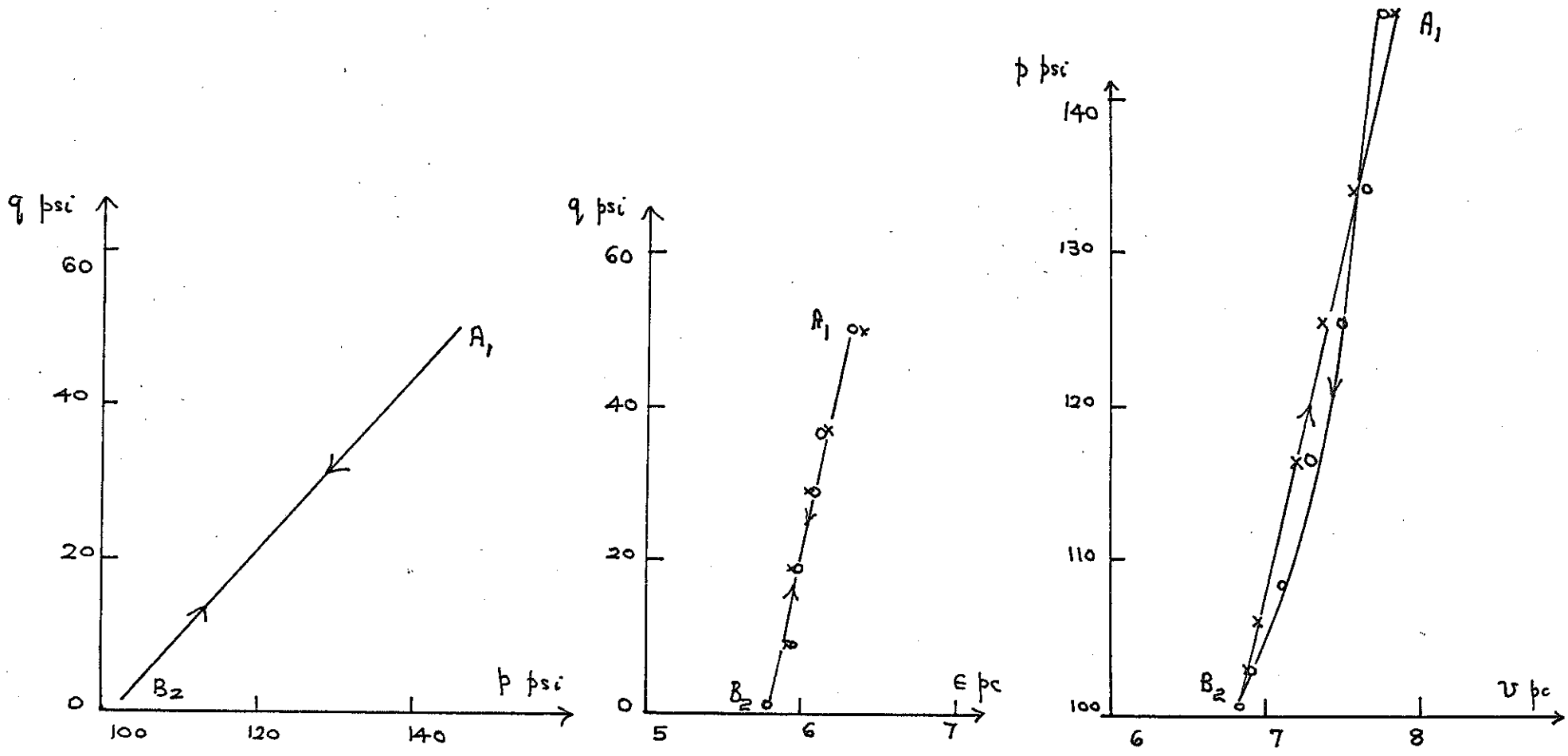

(a) The stress path followed by specimen CG.

(b) The (q , ϵ) relation

(c) The (p , v) relations.

Fig. 6·86. The (q , ϵ) and (p , v) characteristics of specimen CG during unloading and reloading.

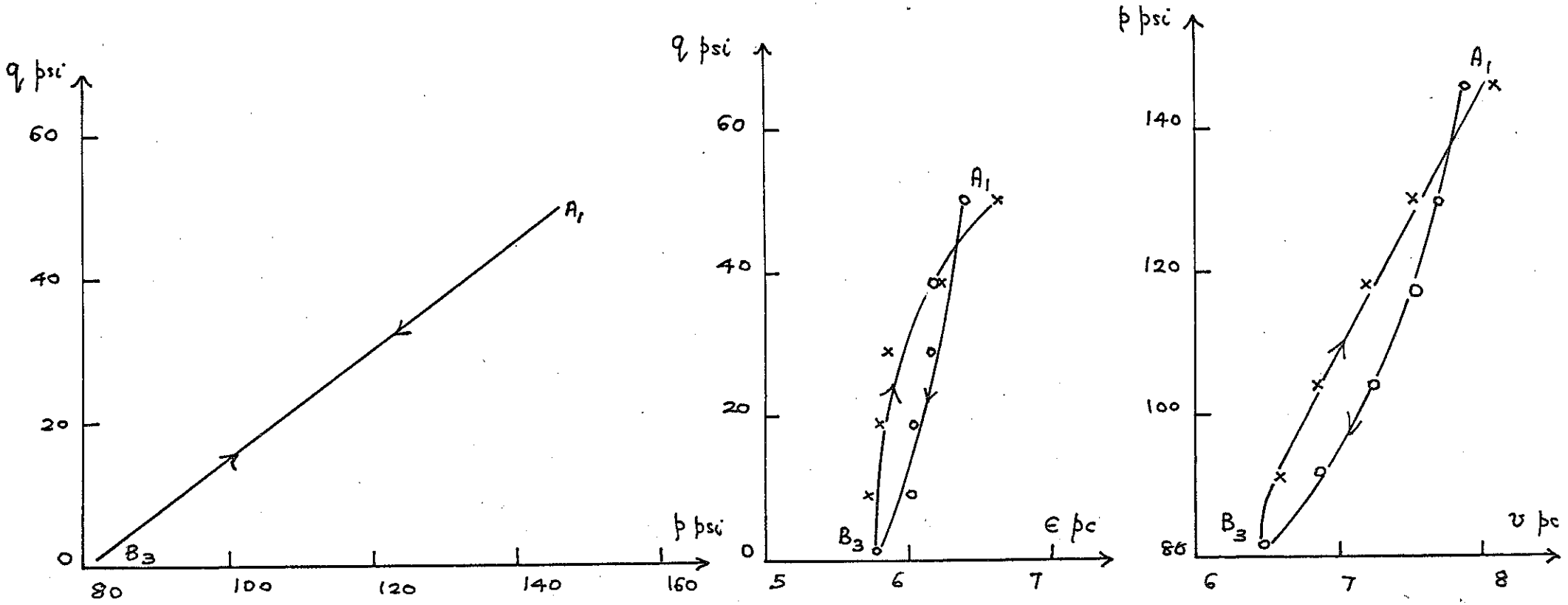

(a) The stress path followed by specimen CG. (b) The (q, ϵ) relation (c) The (p, v) relation.

Fig.6.87. The (q, ϵ) and (p, v) characteristics of specimen CG during unloading and reloading.

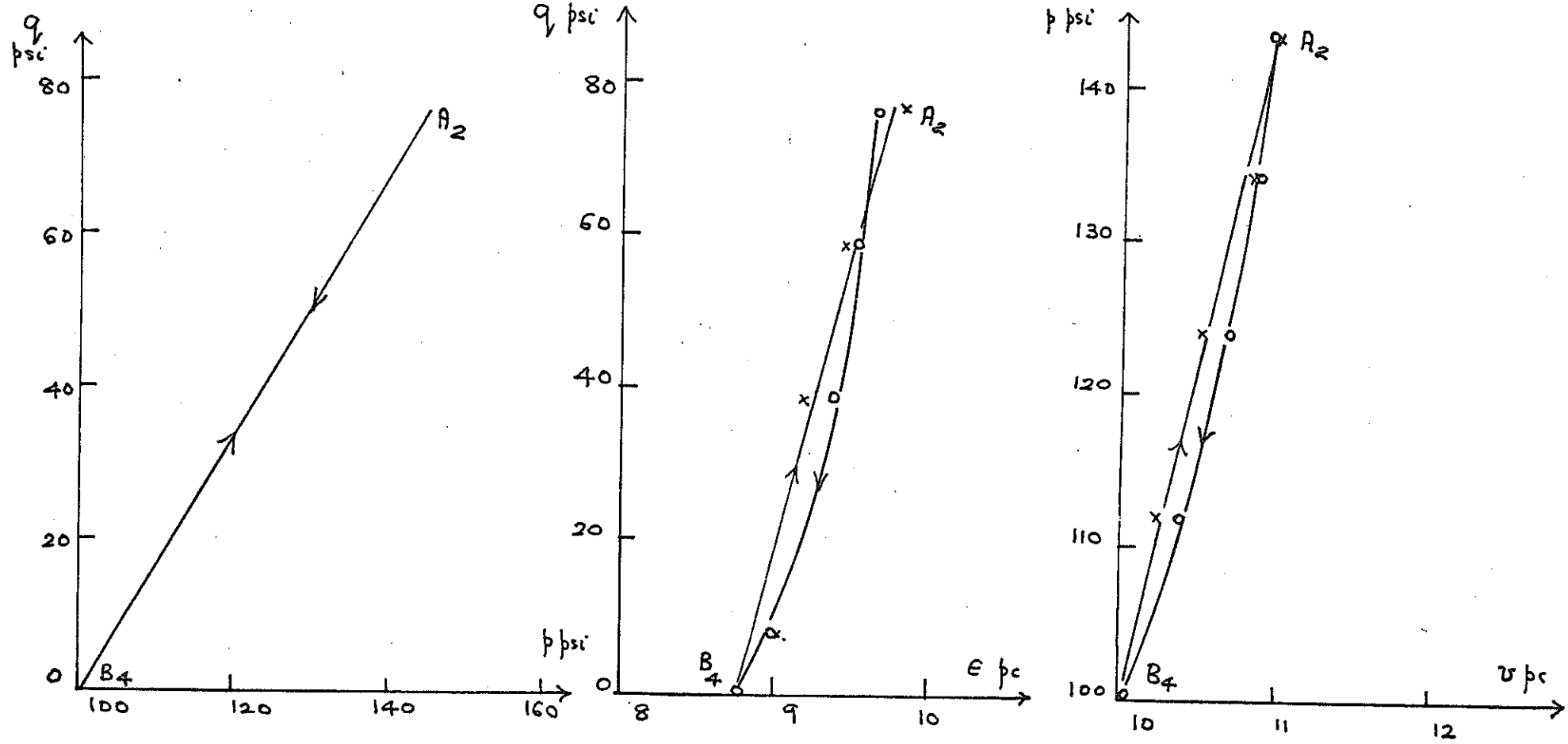

(a) The stress path followed by specimen CG (b) The (q , ϵ) relation. (c) The (p , v) relation

Fig. 6.88. The (q , ϵ) and (p , v) characteristics of specimen CG during unloading and reloading.

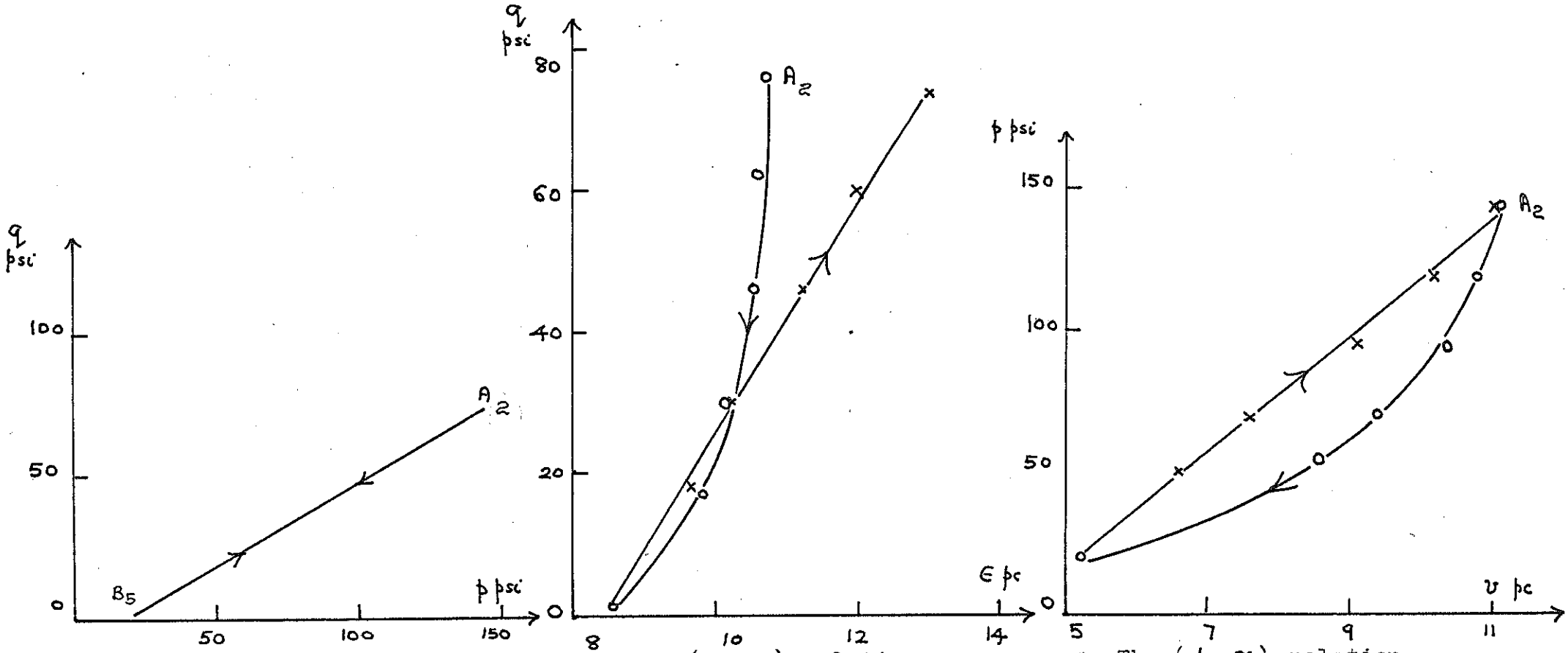

Fig. 6.89. The (q, ϵ) and (p, v) characteristics of specimen CG during unloading and reloading.

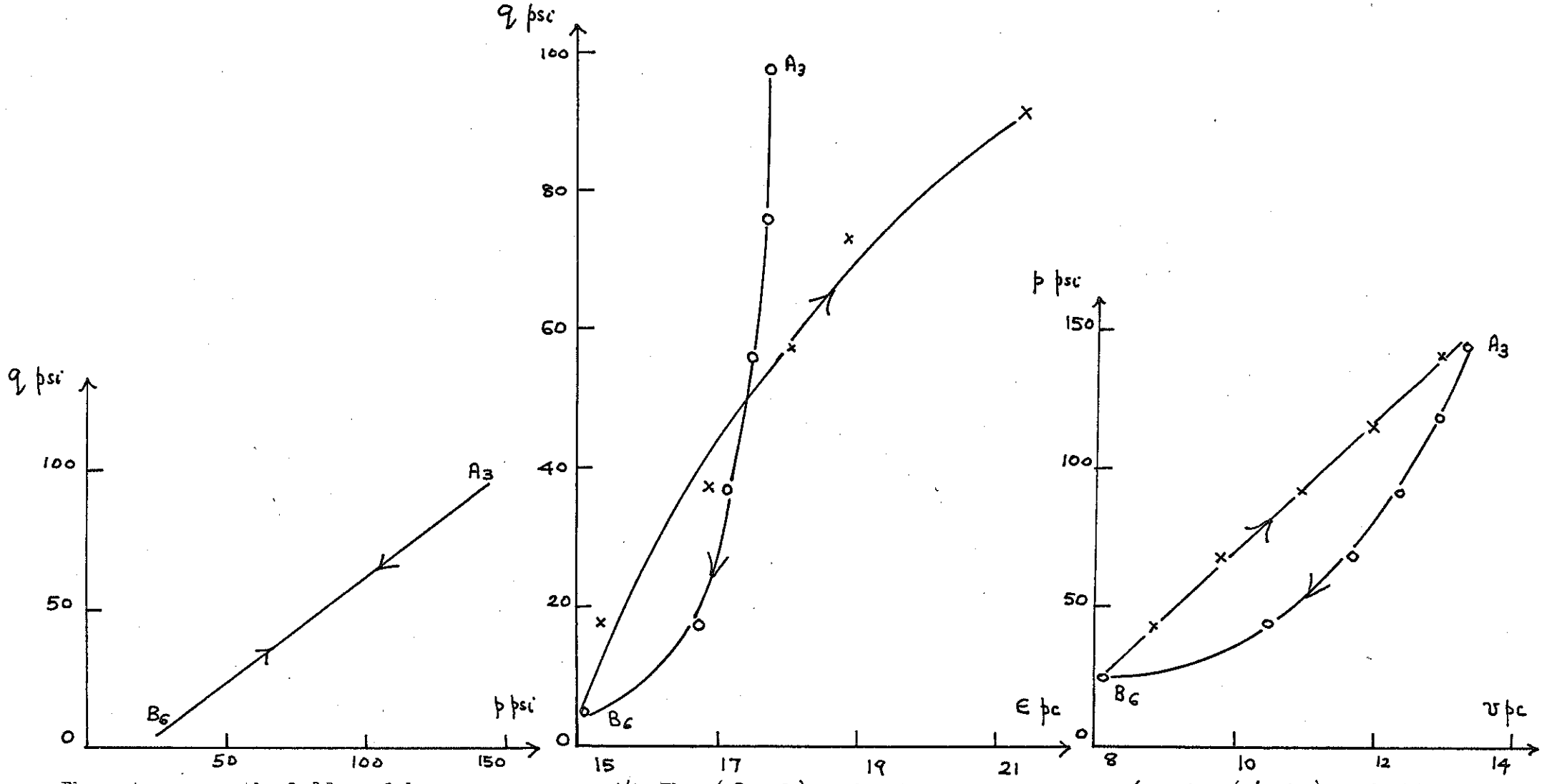

(a) The stress path followed by specimen CG.

(b) The (q, ϵ) relation

(c) The (p, v) relation

Fig. 6.90 The (q, ϵ) and (p, v) characteristics of specimen CG during unloading and reloading.

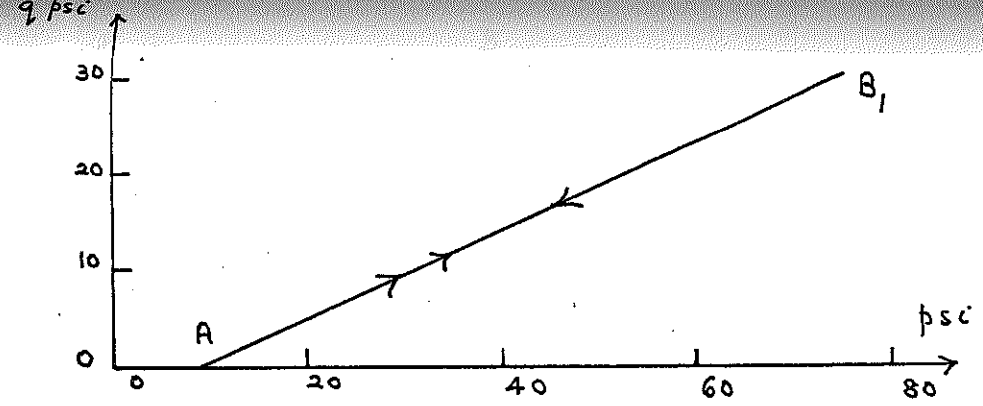

(a) The stress path followed by the heavily overconsolidated specimen T_{I9}

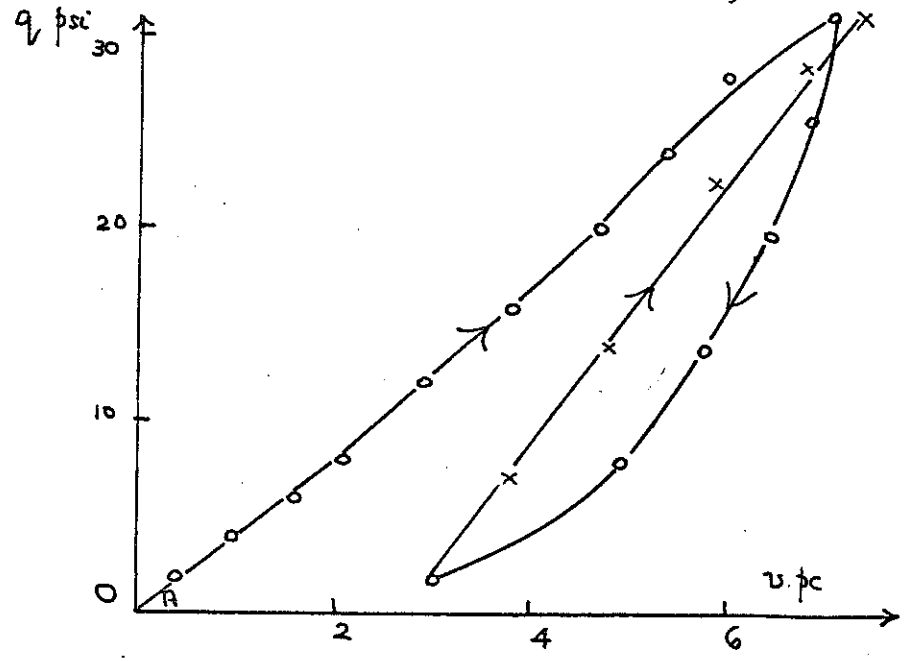

(c) The (q , v) relation

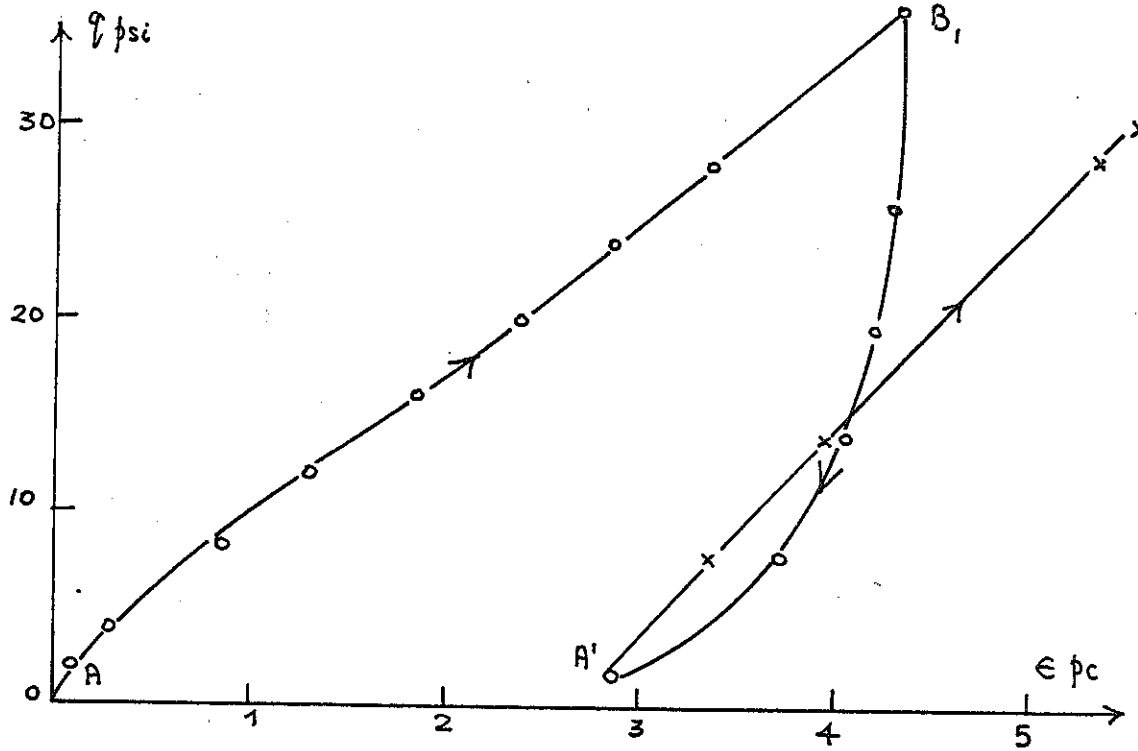

(b) The (q , ε) relation

Fig.6.91. The (q , v) and (q , ε) characteristics of the heavily overconsolidated specimen T_{I9}

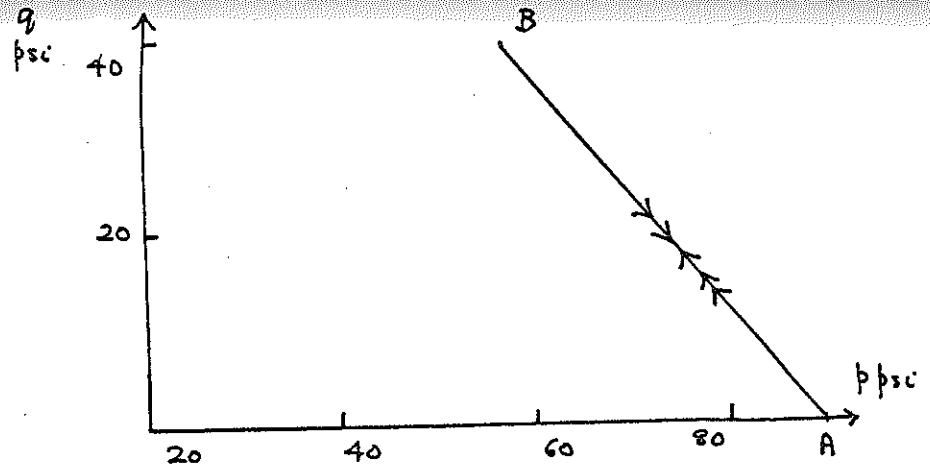

The stress path followed by specimen BU.

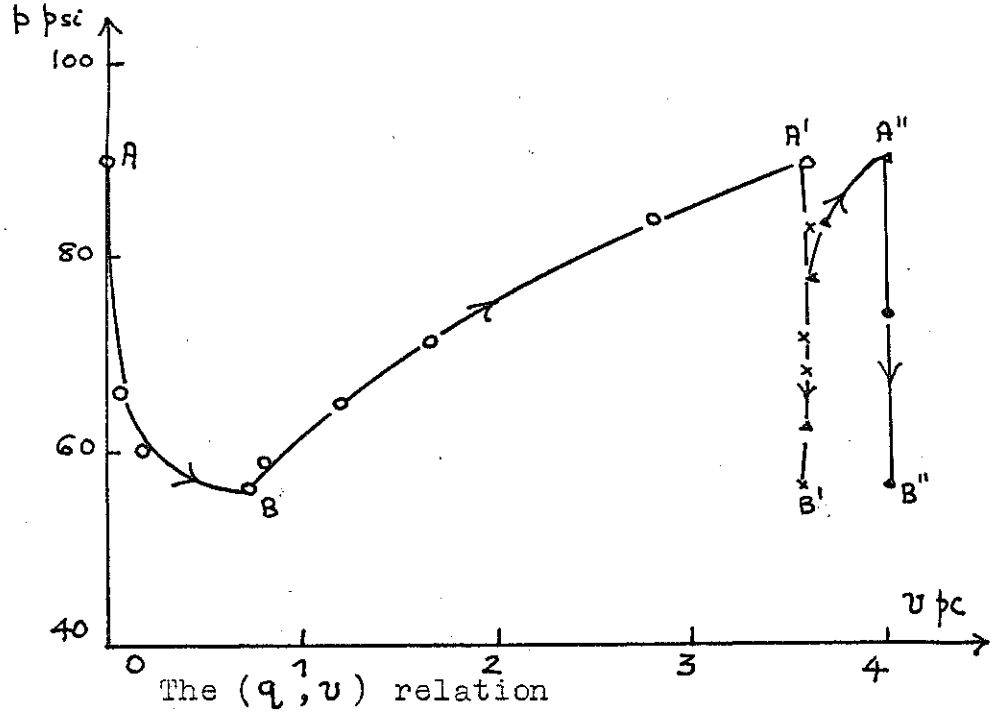

The (q, v) relation

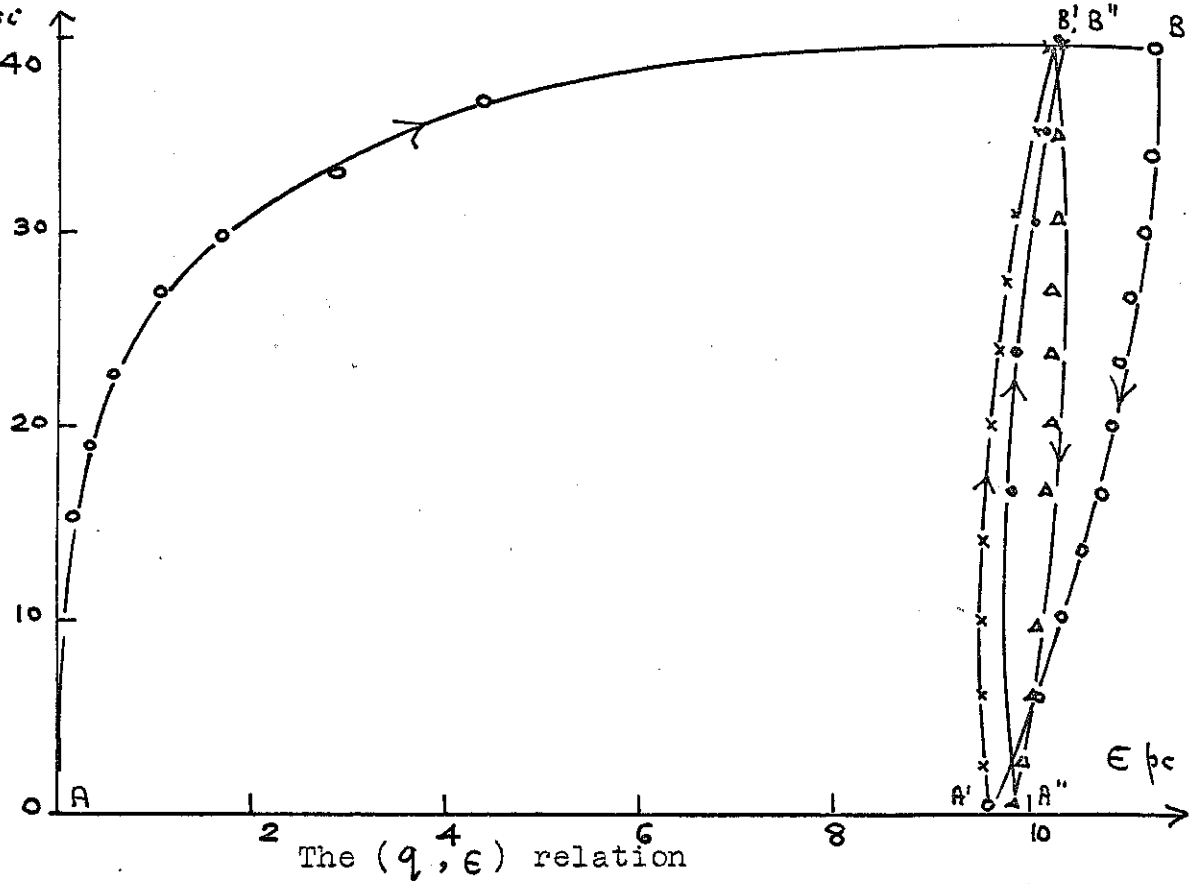

The (q, ε) relation

Fig.6.92. The (q, v) and (q, ε) characteristics of specimen BU.

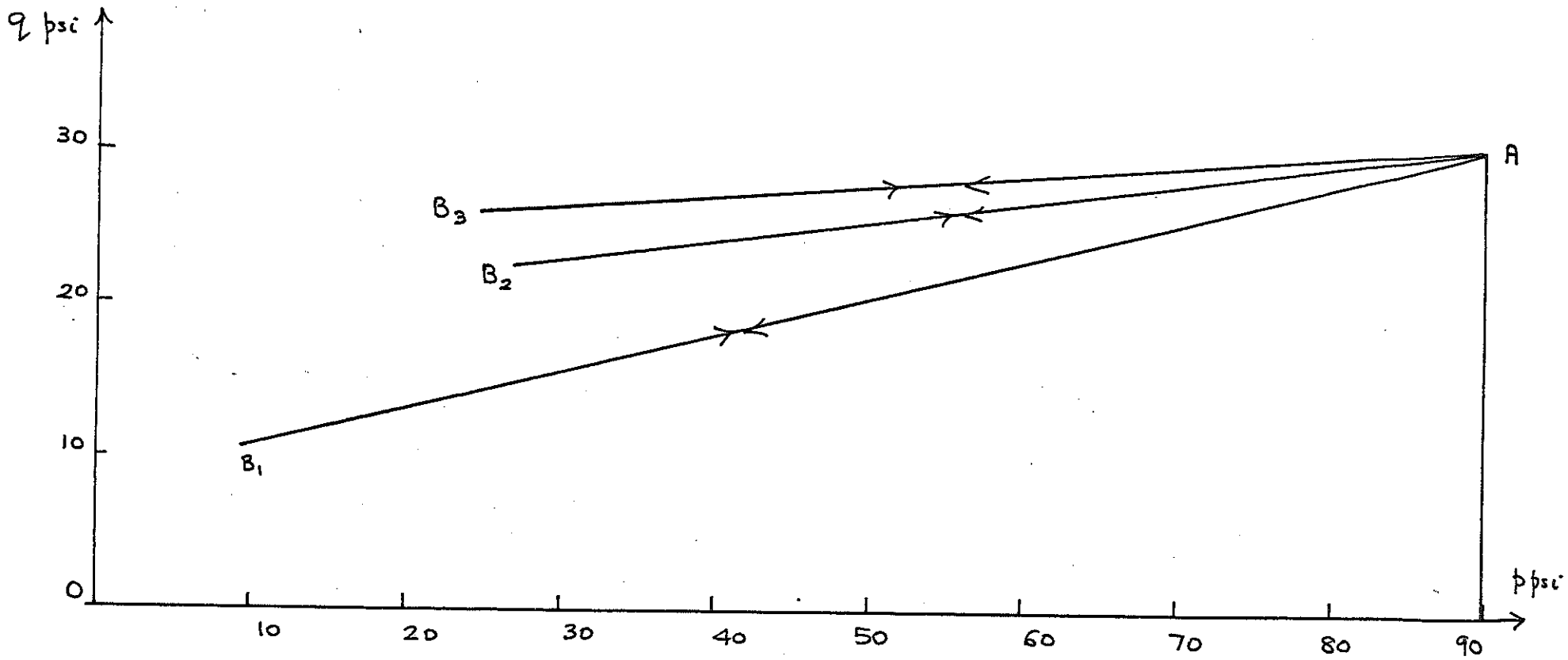

Fig. 6.93(a) The stress path followed by specimen T_{I7}.

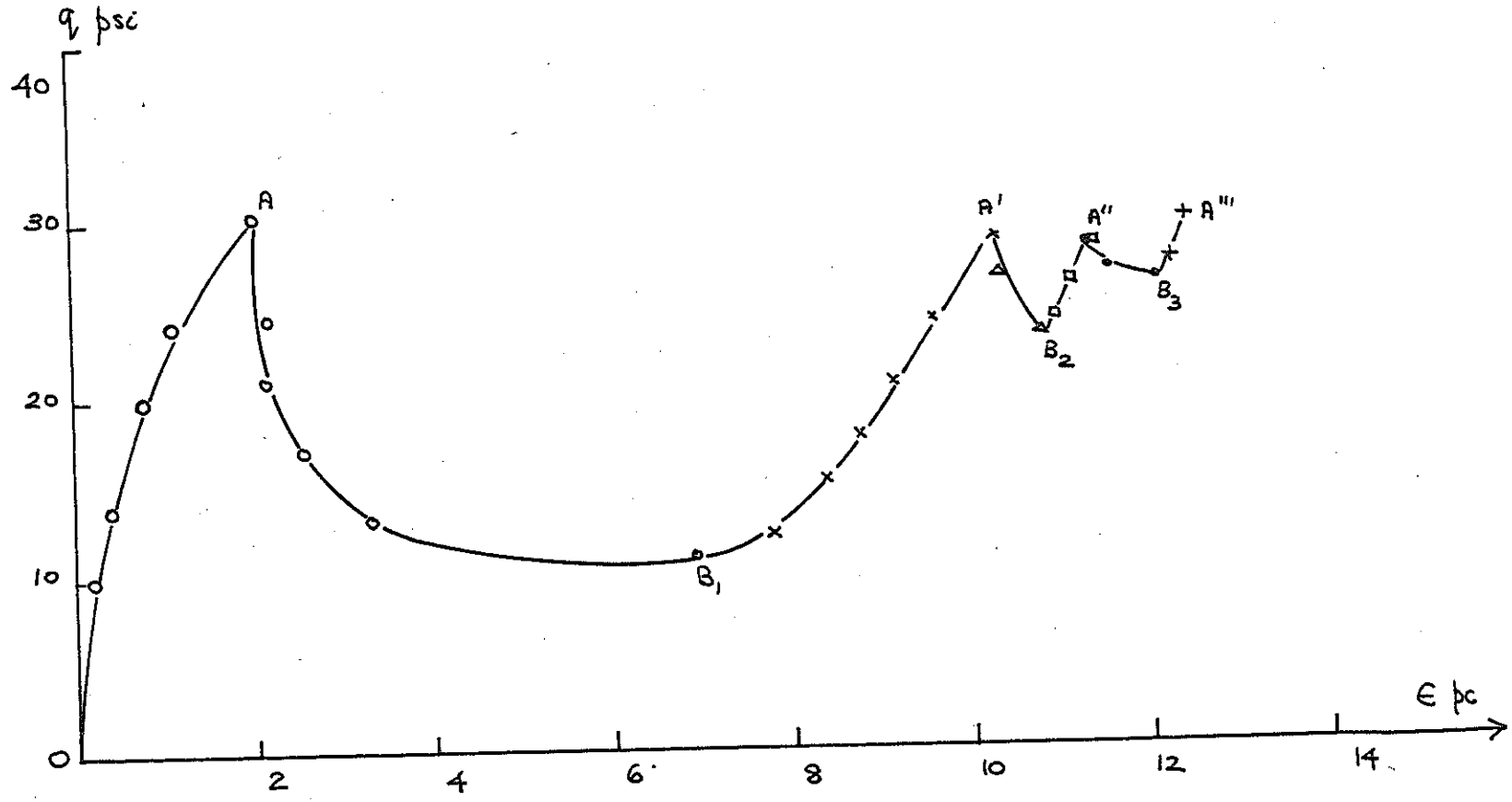

Fig. 6.93(b) The (q, ϵ) characteristic of specimen during cyclic loading.

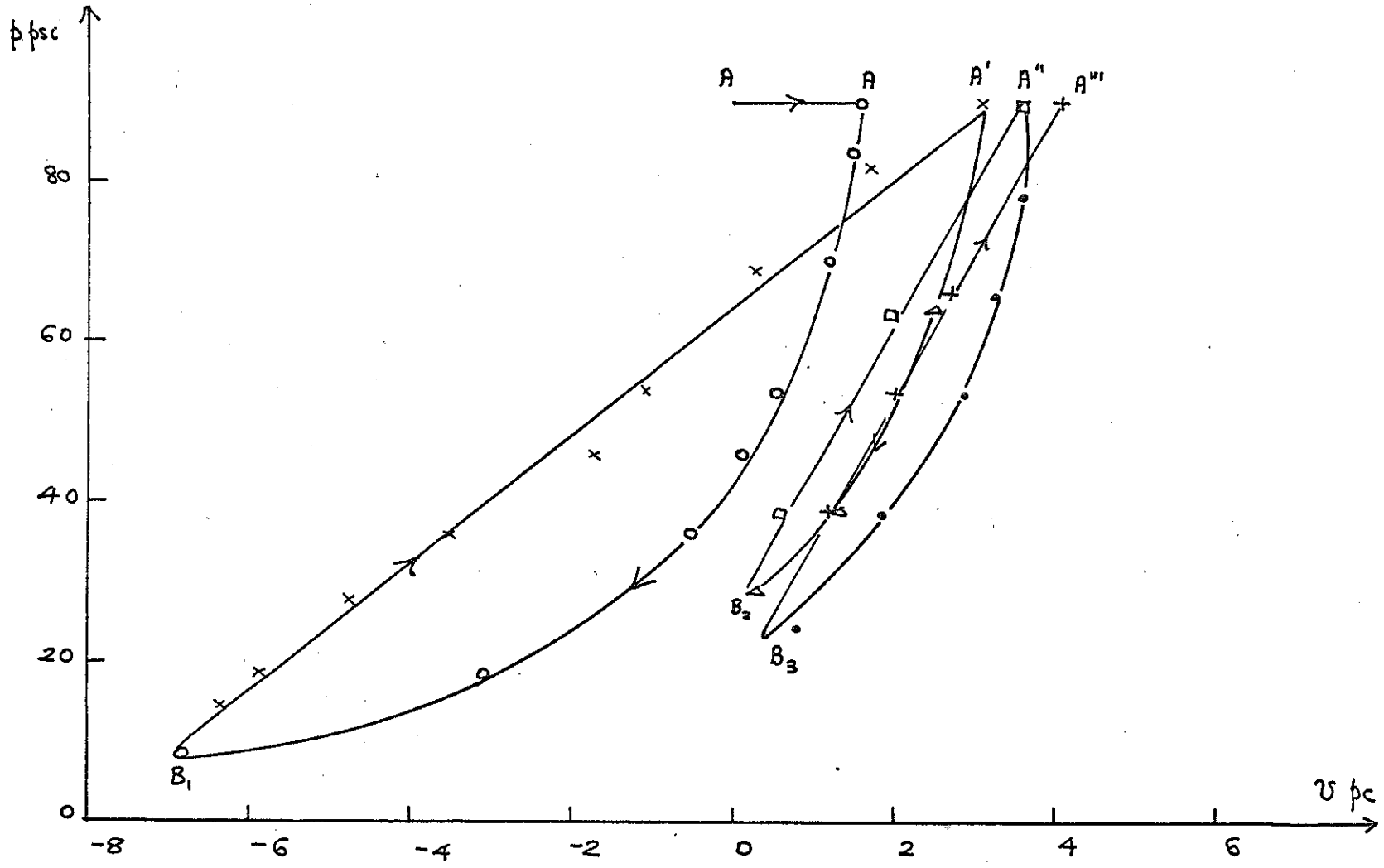

Fig. 6·93(c) The (p, v) characteristic of specimen T_{I7} during cyclic loading.

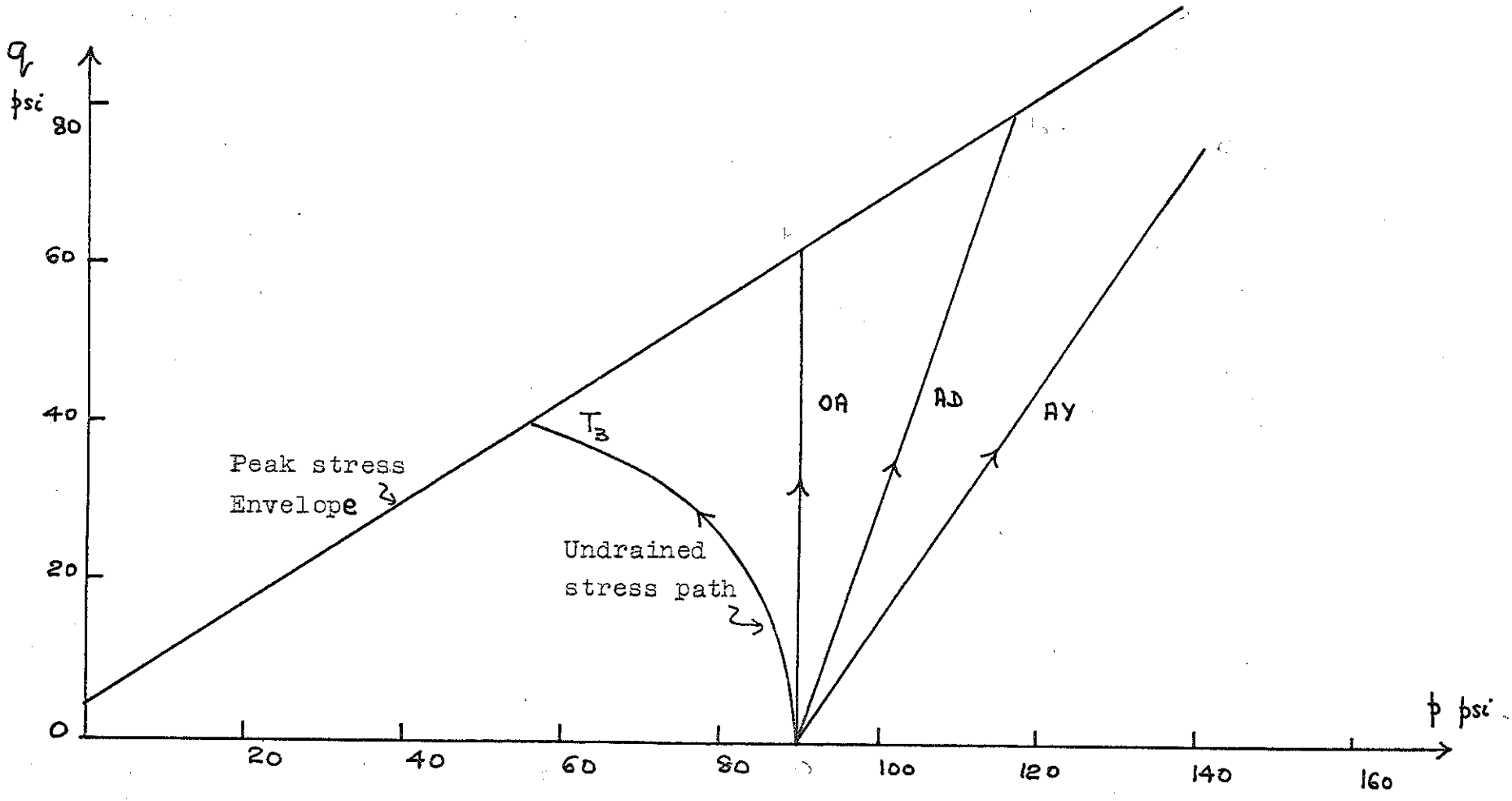

Fig. 7.1. The stress paths followed by specimens OA,AD and AY in GroupI tests.

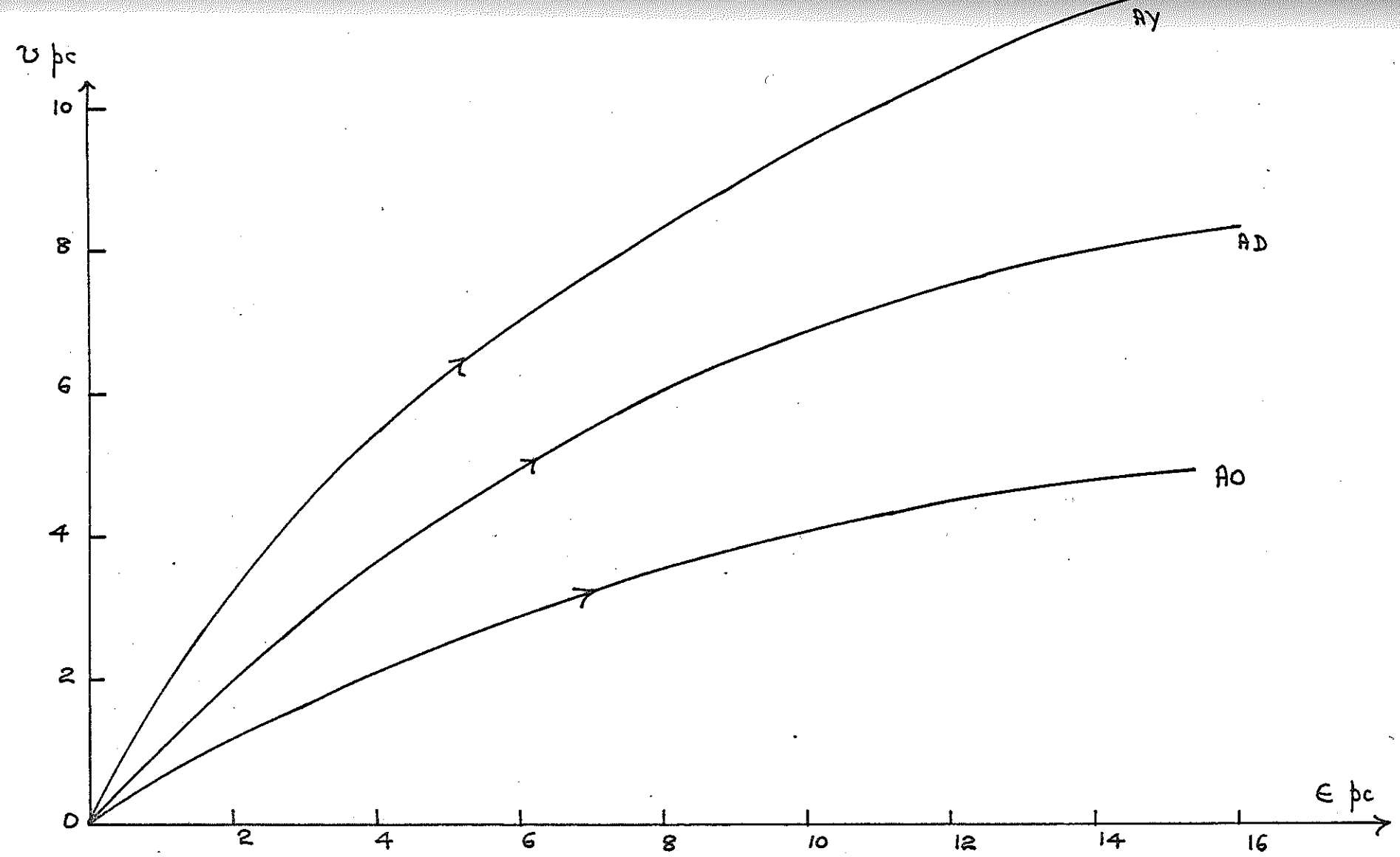

Fig. 7.2. The (υ, ϵ) characteristics of specimens AO, AD and AY sheared along Group I test Paths.

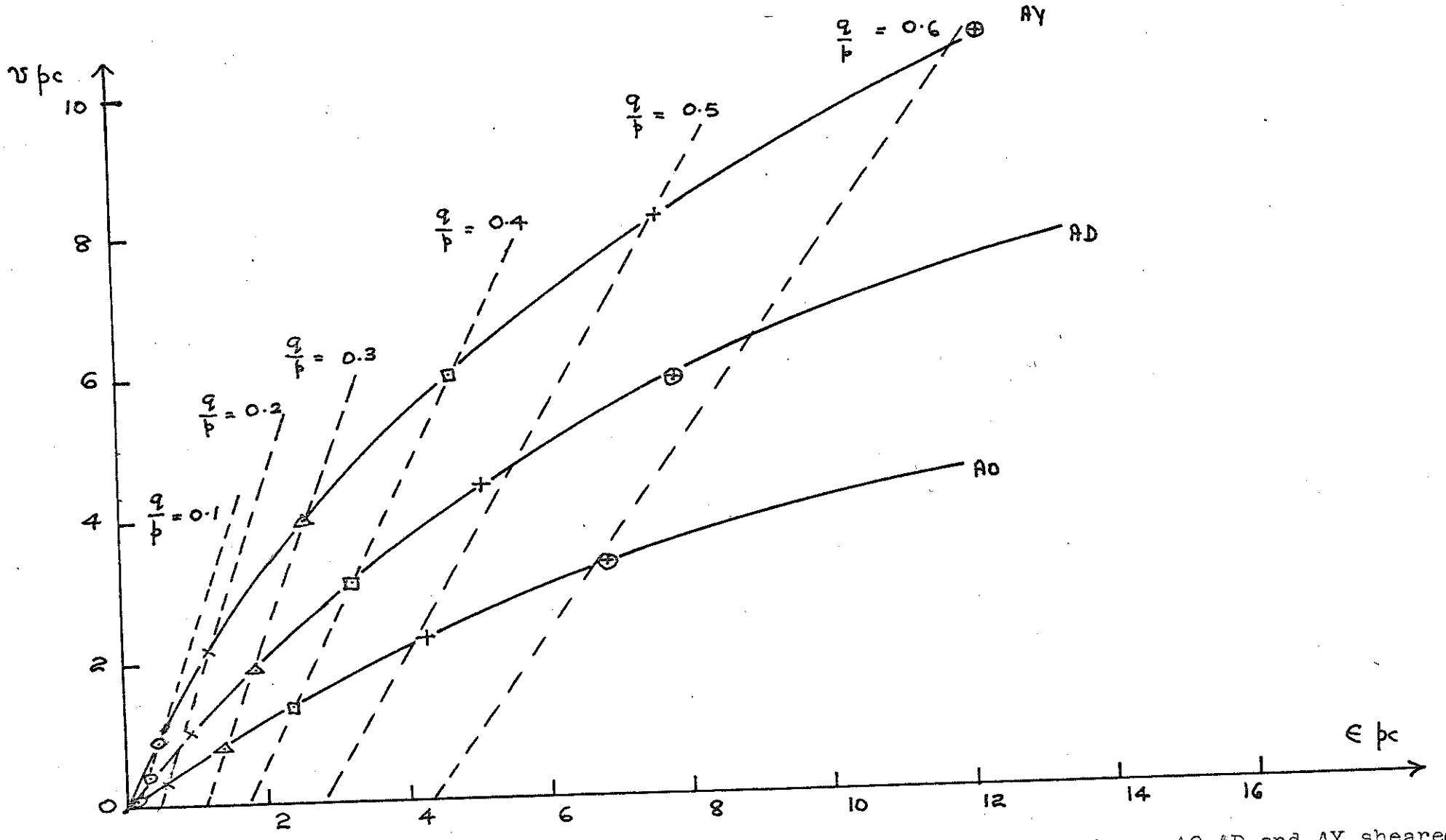

Fig. 7.3. Contours of constant q/p on the (υ , ϵ) characteristics of specimens AO, AD and AY sheared along Group I test paths.

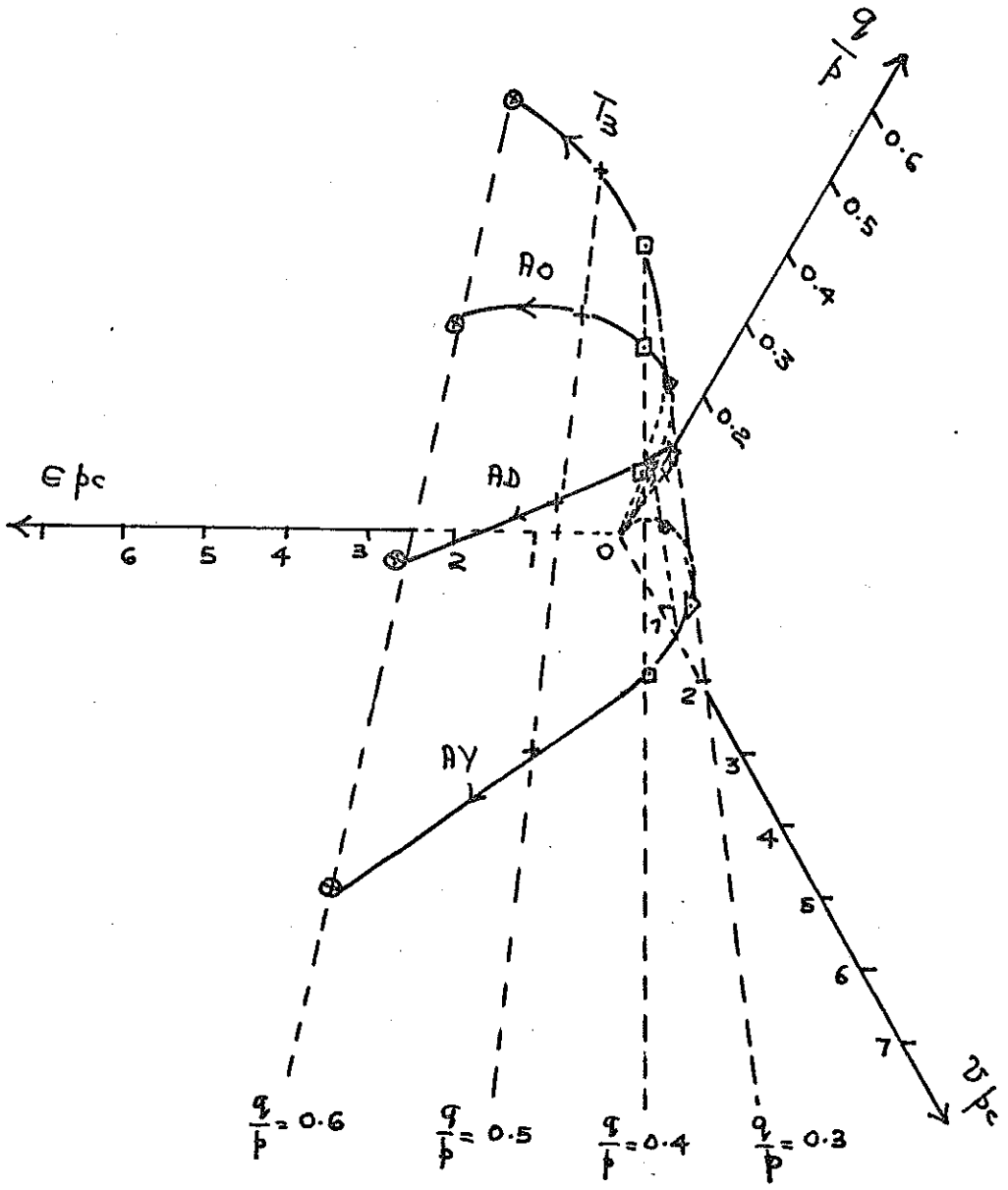

Fig. 7.4(a) The paths followed by specimens T_3, AO, AD and AY In the $(\frac{q}{p}, v, \epsilon)$ space.

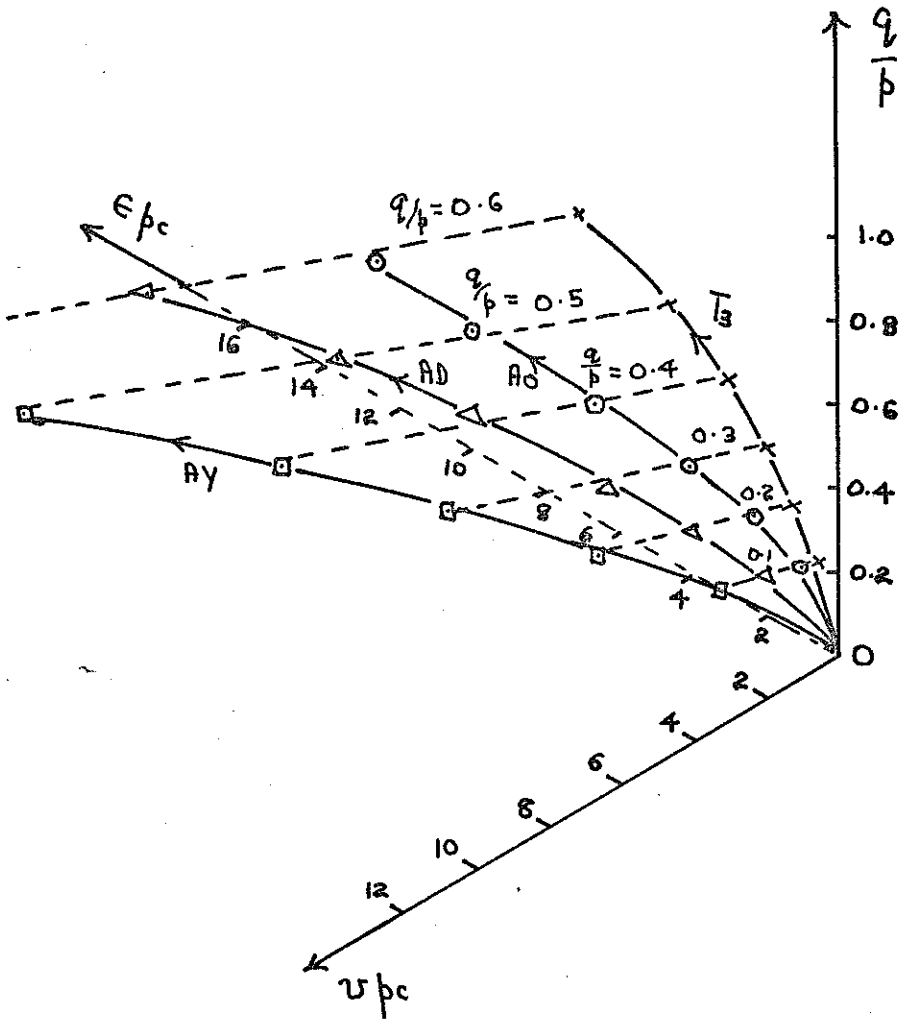

Fig. 7.4(b) The paths followed by specimens T_3, AO, AD, and AY in the $(\frac{q}{p}, v, \epsilon)$ space.